2D VS 3D MODELS FOR THE SEISMIC RESPONSE ASSESSMENT OF REINFORCED CONCRETE FRAMED STRUCTURES

A THESIS SUBMITTED TO
THE FACULTY OF ARCHITECTURE AND ENGINEERING
OF
EPOKA UNIVERSITY

BY

KLEA KASA

IN PARTIAL FULFILLMENT OF THE REQUIREMENTS
FOR
THE DEGREE OF MASTER OF SCIENCE
IN
CIVIL ENGINEERING

JUNE, 2024

`

Approval sheet of the Thesis

This is to certify that we have read this thesis entitled **"2D vs 3D Models for the Seismic Response Assessment of Reinforced Concrete Framed Structures"** and that in our opinion it is fully adequate, in scope and quality, as a thesis for the degree of Master of Science.

_____

Assoc. Prof. Dr. Mirjam Ndini
Head of Department
Date: June, 25, 2024

Examining Committee Members:

Prof. Dr. Hüseyin Bilgin	(Civil Engineering)	_____
Assist. Prof. Dr. Mirjam Ndini	(Civil Engineering)	_____
Dr. Marsed Leti	(Civil Engineering)	_____

`

I hereby declare that all information in this document has been obtained and presented in accordance with academic rules and ethical conduct. I also declare that, as required by these rules and conduct, I have fully cited and referenced all material and results that are not original to this work.

Name Surname: Klea Kasa

Signature: _____

`

ABSTRACT

2D VS 3D MODELS FOR THE SEISMIC RESPONSE ASSESSMENT OF REINFORCED CONCRETE FRAMED STRUCTURES

Kasa, Klea

M.Sc., Department of Civil Engineering

Supervisor: Prof. Dr. Hüseyin Bilgin

Earthquakes are serious threat to human lives and infrastructure. The earthquake the struck Albania in November 2019, where 51 people lost their lives and thousands got injured, is a reminder of the tragic impact that the seismic events have on the community. Proper seismic designing of structures on earthquake-prone countries is very important. Engineers aspire new designing methods that shorten the time and reduce the amount of work. In this context, this study was focused on assessing the seismic behavior of three low-to-mid-rise reinforced concrete buildings, ranging from 5 to 12 stories. These structures were represented using three-dimensional (3D) frame elements in ETABS. Additionally, two-dimensional (2D) models were generated from the internal frames along two orthogonal directions of the 3D models. Using NONLIN software to perform time history analyses, the study compares the displacement demands obtained by nonlinear time history analyses of both 2D and 3D models to explore the reliability of 2D models in reflecting the behavior of their 3D counterparts. The study considers three types of reinforced concrete buildings, 5, 8 and 12 stories, finding that 2D models effectively approximate 3D model behavior, with average roof drift differences of 0.18% in both directions for 5-storey building, 0.023% and 0185% in x and y directions for 8-storey building and 0.027% and 0.28% in x and y directions for 12-storey building.

Keywords: *Displacement demand, time history analysis, 2D and 3D models, linear analysis, nonlinear analysis.*

`

ABSTRAKT

VLERËSIMI I PERFORMANCËS SIZMIKE TË NDËRTESAVE BETONARME 2D VS 3D

Kasa, Klea

Master Shkencor, Departamenti i Inxhinierisë së Ndërtimit

Udhëheqësi: Prof. Dr. Hüseyin Bilgin

Tërmetet janë një kërcënim serioz për jetët njerëzore dhe infrastrukturën. Tërmeti që goditi Shqipërinë në nëntor 2019 është një kujtesë e ndikimit tragjik që ngjarjet sizmike kanë në komunitet. Projektimi i duhur sizmik i strukturave në vendet e prirura për tërmete është shumë i rëndësishëm. Inxhinierët aspirojnë metoda të reja projektimi që shkurtojnë kohën dhe zvogëlojnë sasinë e punës. Në këtë kontekst, ky studim u përqendrua në vlerësimin e sjelljes sizmike të tre ndërtesave prej betoni të armuar me lartësi të ulët deri në mesatare, duke filluar nga 5 deri në 12 kate. Këto struktura u përfaqësuan duke përdorur elemente kornizë tridimensionale (3D) në ETABS. Për më tepër, modelet dy-dimensionale (2D) u gjeneruan nga kornizat e brendshme përgjatë dy drejtimeve ortogonale të modeleve 3D. Duke përdorur programin NONLIN për të kryer analizat "time history", studimi krahason kërkesat e zhvendosjes të marra nga analizat "time history" jolineare të modeleve 2D dhe 3D për të eksploruar besueshmërinë e modeleve 2D në reflektimin e sjelljes së homologëve të tyre 3D. Studimi merr në konsideratë tre lloje të ndërtesave prej betoni të armuar, 5, 8 dhe 12 kate, duke gjetur se modelet 2D përafrojnë në mënyrë efektive sjelljen e modelit 3D, me diferenca mesatare të zhvendosjes së çatisë prej 0,18% në të dy drejtimet për ndërtesën 5-katëshe, 0,023% dhe 0,0185% në drejtimet x dhe y për ndërtesën 8-katëshe dhe 0.027% dhe 0.28% në drejtimet x dhe y për ndërtesën 12-katëshe.

Fjalët kyçe: *Kërkesa e zhvendosjes, analiza "time history", modele 2D dhe 3D, analiza lineare, analiza jolineare*

`

To my family, whose endless support and encouragement have been the foundation of my every achievement.

`

ACKNOWLEDGEMENTS

I would like to express my deepest gratitude to my supervisor, Professor Hüseyin Bilgin, for his guidance, feedback, and constant support throughout this journey.

A huge shoutout to my best friend for getting me into civil engineering. Without her, I wouldn't be here today finishing this thesis, the best decision I've ever made! Suela, this one is for you!

`

TABLE OF CONTENTS

ABSTRACT iii

ABSTRAKT iv

ACKNOWLEDGEMENTS vi

LIST OF TABLES x

LIST OF FIGURES xi

CHAPTER 1 1

INTRODUCTION 1

1.1 General 1

1.2 Thesis objectives 2

1.3 Scope of work 2

1.4 Organization of the thesis 3

CHAPTER 2 5

LITERATURE REVIEW 5

2.1 Seismic Analysis Methods 5

2.2 Linear Analyses 6

2.2.1 Linear Static Analysis 6

2.2.2 Linear Dynamic Analysis 7

2.3 Nonlinear Analyses 10

2.3.1 Nonlinear Static Analysis 10

2.3.2 Nonlinear Dynamic Analysis 16

2.4 Pushover Analysis vs. Time History Analysis 18

`

2.5 Computational tools in structural analysis 19

2.5.1 Overview of software in Structural Engineering 19

2.5.2 ETABS Software 19

2.5.3 NONLIN Software 20

CHAPTER 3 22

METHODOLOGY 22

3.1 Introduction to methodology 22

3.2 Pushover Analysis using ETABS 22

3.2.1 Plastic Hinges Installation 23

3.2.2 Load Application 23

3.3 Bilinearization of Capacity Curves 24

3.4 Nonlinear Time History Analysis using NONLIN 26

CHAPTER 4 29

CASE STUDY 29

4.1 Description of Building Models 29

4.2 Development of 2D and 3D models 33

4.2.1 3D Modeling 33

4.3.2 2D Modeling 35

4.3 Pushover Analysis Procedure 36

4.3.1 Plastic Hinges Installation 36

4.3.2 Load Application 37

4.3.3 Analysis Execution 39

`

4.4 Time History Analyses Procedure 41

4.4.1 Bilinearization Process 41

4.4.2 Nonlinear Time History Analyses 43

4.5 Results and discussions 46

CHAPTER 5 50

CONCLUSIONS 50

5.1 Conclusions 50

5.2 Recommendations for future research 51

APPENDIX 55

`

LIST OF TABLES

Table 1: Seismic analysis methods [5] 5

Table 2: Key characteristics of buildings modeled in ETABS 31

Table 3: 5-Sorey Building, Periods and Weights in X and Y directions 38

Table 4: 8-Sorey Building, Periods and Weights in X and Y directions 38

Table 5: 12-Sorey Building, Periods and Weights in X and Y directions 38

Table 6: Parameters used for Time History Analysis 42

Table 7: Parameters used for Time History Analysis 42

Table 8: Far-Field Records, Roof Drift Demands of 3D 5-, 8-, 12-storey building models (%) 44

Table 9: Far-Field Records, Roof Drift Demands of 2D 5-, 8-, 12-storey building models (%) 45

Table 10: Near-Field Records, Roof Drift Demands of 3D 5-, 8-, 12-storey building models (%) 45

Table 11: Near-Field Records, Roof Drift Demands of 2D 5-, 8-, 12-storey building models (%) 46

Table 12: Maximum and average roof drift values for 3D models in both directions (%) 47

Table 13: Maximum and average roof drift values for 2D models in both directions (%) 47

Table 14: Parameters used to perform nonlinear time histroy analyses on NONLIN 55

Table 15: Roof Drift Demand (%) for 3D building models 59

Table 16: Roof Drift Demand (%) for 2D building models 62

`

LIST OF FIGURES

Figure 1: Representation of Equivalent Lateral Force Method [7] 7

Figure 2: Example of elastic response spectrum [9] 8

Figure 3: Peak Ground Acceleration shown on Accelerogram [10] 9

Figure 4: Capacity Curve obtained by Pushover Analysis [12] 11

Figure 5: Nonlinear Static Procedure [11] 12

Figure 6: Moment-Rotation relationship [11] 13

Figure 7: Force-Deformation relation for Concrete Components [14] 14

Figure 8: Load patterns corresponding to higher modes [11] 15

Figure 9: Performance evaluation graph [11] 15

Figure 10: Multi-record IDS curve for a 5-storey building [16] 17

Figure 11: Bilinear Force-Deformation Relationship in SDOF Model [4] 21

Figure 12: Pushover Curve Bilinearization [20] 24

Figure 13: Transformation of MDOF to SDOF [22] 26

Figure 14: Input parameters for nonlinear analysis in NONLIN 27

Figure 15: Plan view of 5-, 8-, and 12-storey building [24] 30

Figure 16: Corner (left) and inner (right) column cross-sections for 5-, 8- and 12-storey buildings [24] 32

Figure 17: Load distribution on two-way slabs of selected buildings [24] 34

Figure 18: The selected 2D frames [24] 35

`

Figure 19: Plastic hinges assigned on ETABS 36

Figure 20: Load Cases used for performing the analyses 37

Figure 21: Base Shear vs. Roof Displacement 40

Figure 22: Base Shear / Seismic Weight vs. Roof Drift Curve 40

Figure 23: Bilinearization of Pushover Curve 3D 5-Storey Building (X-Direction) . 41

Figure 24: Running the analysis in NONLIN 43

Figure 25: Average Roof Drift (%) 48

Figure 26: Maximum Roof Drift (%) 48

CHAPTER 1

INTRODUCTION

1.1 General

In regions with high seismic activities, the safety of buildings is predominant. Earthquakes are serious threat to human lives and also infrastructure, so buildings that withstand these ground motions are necessary. 6.4 magnitude earthquake that struck Albania in November 2019, where 51 people lost their lives and 3000 others got injured [1], is a reminder of the terrible effect that seismic events have on community. This earthquake has not only resulted in tragic losses of lives, but also created a lot of damage to infrastructure, leaving behind many totally collapsed or unsafe buildings. Fast forward to 2023, Turkey experienced two catastrophic seismic events, which happened at intervals of nine hours. These earthquakes affected 14 million people, with a death toll of over 50000 individuals. The total cost of earthquake damage was over USD 104 billion [2].

These recent earthquakes highlight the importance of a great design and the need for more efficient seismic analysis methods in construction. Among the existing buildings, low and medium height reinforced concrete buildings take a significant part on Albanian building stock. Therefore, understanding the behavior of these buildings under earthquake loading is very important. The loss of lives and financial damage resulting from earthquakes in Albania, Turkey and other countries, stresses the importance of seismic performance evaluation of buildings.

The process of designing earthquake-resistant structures is very long. Design professionals are using different tools to perform seismic analysis. When designing the building traditionally in software, usually it can be time-consuming and non-profitable due to the complexity of the building. For this reason, engineers tend to reach out new methods to make a quicker and cost-effective construction. This study addresses the need to evaluate whether 2D frame models can accurately reflect the seismic behavior of their corresponding 3D frames. When using new shorter methods for designing

`

structures, we should not compromise on their safety. The structures not only should withstand the test of time, but also the unpredictability of nature.

1.2 Thesis objectives

This study aims to evaluate whether 2D frame models can accurately reflect the seismic behavior of their 3D counterparts. This includes a careful consideration of modeling and precision in predicting how buildings will respond to seismic forces. Three frame buildings, 5-, 8-, and 12-storey each, have been considered for the analysis. The displacement demands of each building are determined using Time History Analysis. The effectiveness of 2D models in representing 3D structures is examined by comparing their displacement demand of 2D nonlinear models against 3D nonlinear models. This means checking if the 2D model seismic results differ from 3D model results.

Achieving these objectives ensures reliability for the use of 2D frame models in seismic analysis and can lead to more efficient and cost-effective design and assessment practices in structural engineering.

1.3 Scope of work

This study focuses on evaluating the seismic performance of various building typologies under near-field and far-field earthquakes. The typologies considered for this study were 3D models of 5-, 8- and 12-storey buildings, as well as their corresponding 2D frame models in both x and y directions. Nonlinear static and dynamic analysis were performed during this study to compare 2D and 3D frame models, using the following software:

- ETABS [3]
- NONLIN [4]

`

Modelling and Static Pushover Analyzes were performed using ETABS. Each 3D model consists of two 2D models, one on both x- and y-direction. Two capacity curves were obtained for each 3D building model, and one capacity curve for each 2D building model, resulting on a total of 12 capacity curves.

Time History Analyses were performed using NONLIN. A total of 146 earthquakes provided in the software were selected in order to perform Time History Analyses. From these records, 68 were far-field and 78 were near-field earthquakes. They were applied on both principal directions of 3D models and on the respective direction of 2D models, in order to compare their displacement demands and how each model responds to different types of seismic records.

1.4 Organization of the thesis

This study will be organized as follows:

- Chapter 1:

  This chapter presents the motive behind the study, raises the problem statement and also summarizes the scope of word. The introduction outlines all the issues that are to be discussed on other chapters of the study.

- Chapter 2:

  This chapter includes a review of existing literature regarding all the issues included on the study. It expresses other researchers' perspective regarding this topic.

- Chapter 3:

  In the methodology section of this study, all the methods and techniques used to conduct the research and to perform each analysis. It also involves all the methods that are used to collect the data and other tools and software used in this study.

`

- Chapter 4:

  Case Study chapter includes a step-by-step representation of all the work and experiments done during the study. This chapter also includes all the results collected from the previous chapters. The outcomes of all the work done are furtherly discussed on this part of the study.

- Chapter 5:

  This chapter restates the importance of the topic and summarizes the study. It also leaves room for comments and recommendation for future research.

`

CHAPTER 2

LITERATURE REVIEW

2.1 Seismic Analysis Methods

The target of structural engineers is to design safe and efficient structures throughout their use. For this reason, they use different analyzing methods to predict the behavior of structures under different loading conditions. Seismic analysis of structures is an important area of study that aims to understand and predict the responses of buildings under earthquake loads.

The analysis of seismic effects on structures is very complex. Structural models can be classified as linear models or nonlinear models and their analyzing methods can be classified according to seismic loading as either being static or dynamic, as shown in *Table 1*. In static analyses a single and constant force is considered, whereas in dynamic analyses the value of this force changes throughout the procedure. Seismic analysis methods are:

STATIC ANALYSIS	• Equivalent Static Analysis • Conventional Pushover Analysis • Adaptive Pushover Analysis
DYNAMIC ANALYSIS	• Multi-Modal Spectral Analysis • Response History Analysis • Incremental Dynamic Analysis

Table 1: Seismic analysis methods ***[5]***

The most reliable and most complex method is Time History Analysis. During this method the behavior of the structure is predicted from data taken from real earthquake events that had happened. Also, it takes more time to complete the procedure compared to other methods.

`

2.2 Linear Analyses

Linear models always have a linear relationship between the applied forces and the resultant displacements. Geometry, cross-sectional properties and material properties will always have a linear relationship between any action and corresponding deformation. When linear methods are used, a response modification factor is taken into account in order to consider the nonlinear behavior of the structures.

2.2.1 Linear Static Analysis

Linear Static Analysis, also known as Equivalent Lateral Force method, is a procedure that puts concentrated static loads on each story level of a structure with specified magnitudes and directions that imitate the effects of dynamic loads caused by earthquakes. These forces tend to occur where concentration of mass on the buildings is the highest, for example of floors and roof. Also, these forces are larger at higher elevations of the structure.

Equivalent Lateral Force method can only be used on structures with low height and regular structure. During this method, the inertial forces are reflected as static forces using empirical formulas. These empirical formulas are used to represent correctly the dynamic behavior of structures that have almost uniform distribution of mass and stiffness. Lateral loads are supposed to represent the future earthquake loading [6]. The shape of the mode on Equivalent Lateral Load Method is almost and inverted triangle.

`

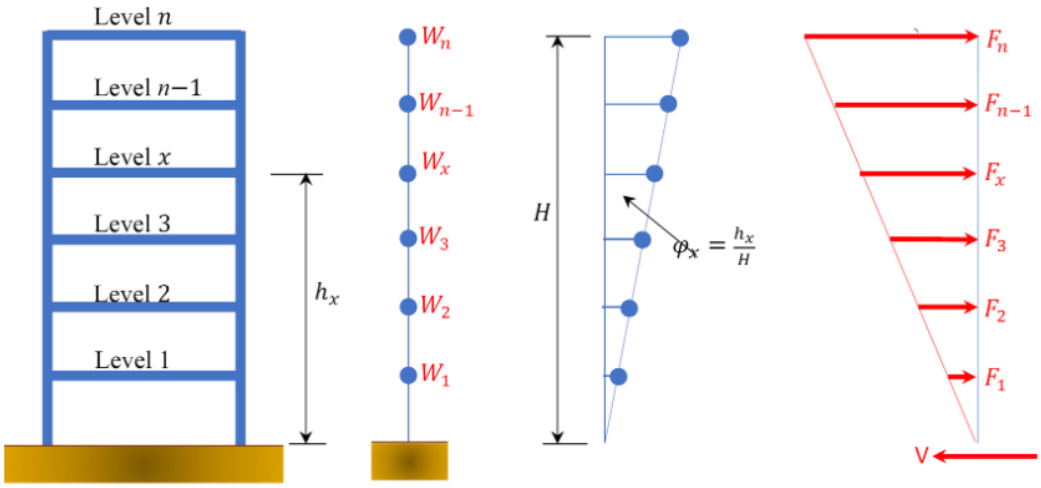

Figure 1: Representation of Equivalent Lateral Force Method ***[7]***

2.2.2 Linear Dynamic Analysis

This method represents an improvement of Linear Static Analysis. This analysis, also known as Response Spectrum Analysis, is a statical analysis used for the determination of the likely response of a structure to seismic loading. [8] Response spectrum shows the maximum response of the structure to a given earthquake. During Time History Analysis, taking into consideration the displacements and forces at every instant time can be very time consuming. For this reason, Response Spectrum Analysis is preferred. [6] The difference between time history and response spectrum is that response spectrum seems to take into consideration maximum response of the equations rather than the full-time history. Response of a structure to ground motion is given by the following dynamic equilibrium equation [5]:

$$\boldsymbol{K\,u(t) + C\dot{u}(t) + M\ddot{u}(t) = M_x\ddot{u}_{gx}(t) + M_y\ddot{u}_{gy}(t) + M_z\ddot{u}_{gz}(t)} \quad (Equation\ 1)$$

Where **K** is the stiffness matrix, **C** is the proportional damping matrix, **M** is diagonal mass matrix, relative displacements, velocities and accelerations are $\boldsymbol{u}, \dot{\boldsymbol{u}}$ and $\ddot{\boldsymbol{u}}$, and $\ddot{\boldsymbol{u}}_{gz}, \ddot{\boldsymbol{u}}_{gy}$ and $\ddot{\boldsymbol{u}}_{gz}$ express the components of uniform ground acceleration. Even though accelerations are obtained in three directions, only the maximum positive one is taken into consideration while performing response spectrum analysis. [8]

`

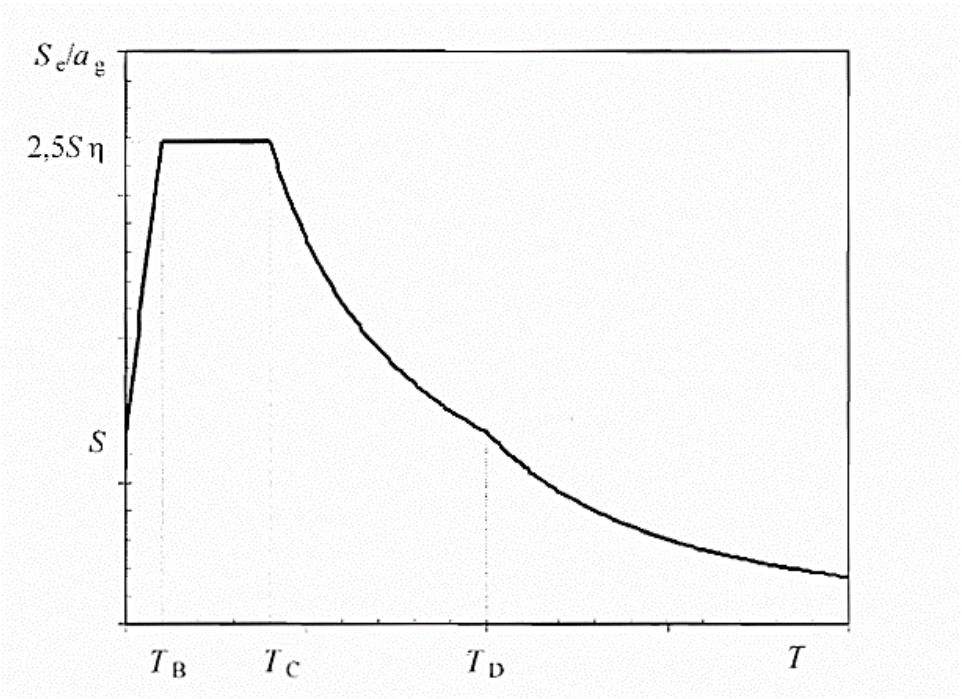

Figure 2: Example of elastic response spectrum ***[9]***

Figure 2 shows an example of elastic response spectrum shape, where:

- T is the vibration period of e linear single degree of freedom system
- a_g is the design ground acceleration
- T_B is the lower limit of the period of the constant part of elastic response spectrum
- T_C is the upper limit of the period of the constant part of elastic response spectrum
- T_D is the period value that defines the beginning of constant displacement response range of the spectrum
- S is the soil factor
- η is damping correction factor [9]

Accelerographs are devices that measure acceleration of rapid ground motion during earthquakes. The data recorded from accelerographs are important for understanding dynamics of earthquakes and for designing structures that are resistant to ground motions. The maximum value we take from an accelerograph is called Peak Ground Acceleration (PGA). Figure 3 shows an example of an accelerogram, with

`

time in seconds plotted on the x-axis and acceleration in cm/s^2 on y-axis. The circeled value shows Peak Ground Acceleration

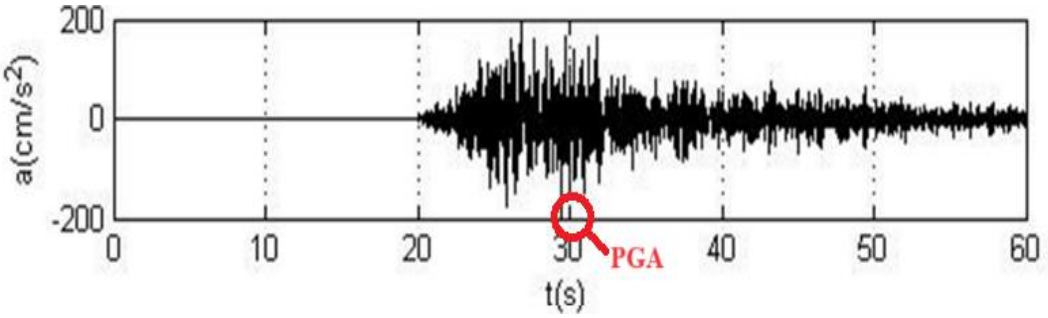

Figure 3: Peak Ground Acceleration shown on Accelerogram ***[10]***

The natural time period of a structure is the time required by a structure to perform a complete free vibration cycle when a force is acted on it. Natural time period (T) depends on the mass (m) and stiffness (k) of the structure. When the mass of the structure increases, the natural period also increases. When the stiffness of the structure increases, the natural time period decreases. PGA is mainly dependent on natural period of the structure. The following equation expresses the relationship between natural period, mass and stiffness of the building [5].

$$T = 2\pi\sqrt{\frac{m}{k}} \qquad (Equation\ 2)$$

When a building is subjected to an earthquake motion, there is a difference in displacement between the base of the building and the roof. This is called the relative displacement of the building and the effect of the earthquake on a structure is dependent on this relative displacement. However, to measure the response of the earthquake, acceleration instead of relative displacement is preferred, because it is easier to obtain the design force (V) [5].

$$Shear\ Force\ (V) = Acceleration\ (a) \times Mass\ (m) \qquad (Equation\ 3)$$

In order to perform Response Spectrum Analysis, it is necessary to design the response spectrum for each earthquake that is expected to happen on a particular

`

location. Then an envelope response spectrum is developed in order to be used in the design. This envelope curve is called the design response spectrum curve and maximum acceleration, spectral acceleration S_a. Design response spectrum is a graph that represents the maximum response like displacement, velocity or acceleration of a single-degree-of-freedom system to earthquake motions, at different natural periods. Parameters of earthquakes influence the shape of response spectra [9],

Response Spectrum and Time History Analysis both assess the seismic demand on structures, but they differ in approach, complexity and the types of results they provide. Since Time History is more complex and requires a lot of time to perform, sometimes response spectrum analysis is recommended. Response spectrum analysis is used for a broad estimation while time history analysis is used for a more detailed and accurate assessment of structural response.

2.3 Nonlinear Analyses

Earthquakes are random and unpredictable events. The load they impose to the building is not linear. Nonlinear seismic analysis methods are advanced techniques used to predict the response of structures under seismic loading. In linear methods it is assumed that the structures respond proportionally to the loads. In nonlinear analysis the changes of material properties, geometry, and boundary conditions that occur during rapid ground motions are taken into account.

2.3.1 Nonlinear Static Analysis

Pushover Analysis is a static, nonlinear seismic analysis method. Performing a damage-controlled design such as static nonlinear analysis, is the best way of reaching performance objectives. This procedure is called static nonlinear analysis because static loads are applied on the structure and some of the elements of this structure are designed using a nonlinear mathematical model [11].

`

The demand and capacity parameter of Pushover Analysis is the lateral displacement of the structure. After preforming the Pushover Analysis on the building, a capacity curve is obtained. The capacity curve is a base shear vs roof displacement graph that defines building capacity for an assumed force distribution [6]. As shown in *Figure 4*, the structure is subjected to a certain load pattern and the roof displacement is measured on each step of this procedure. After a certain value of roof displacement is reached, a curve called Capacity Curve can be plotted, with top displacement in mm on x-axis and base shear in kN on y-axis.

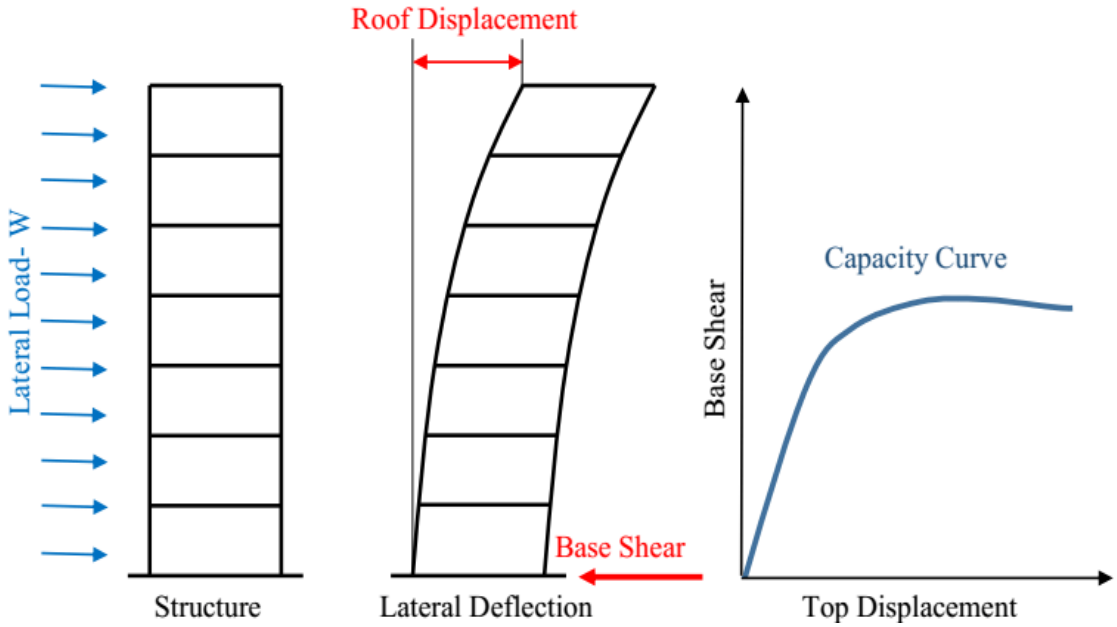

Figure 4: Capacity Curve obtained by Pushover Analysis ***[12]***

The aim of performing Pushover Analysis is to determine the expected performance of a structural system. This is accomplished by estimating strength and deformation demands of the building and comparing them to available capacities at the performance level of interest. Pushover provides information that cannot be obtained by dynamic analysis [13]. The point where demand and capacity curves intersect each other is called the performance point of the structure. It shows the maximum displacement that the building can undergo during an earthquake event. To implement Pushover Analysis procedure, four phases should be followed [9]:

1. Defining the structural model

`

2. Selecting the load pattern to define the capacity of the structure
3. Defining the seismic demand
4. Building performance evaluation

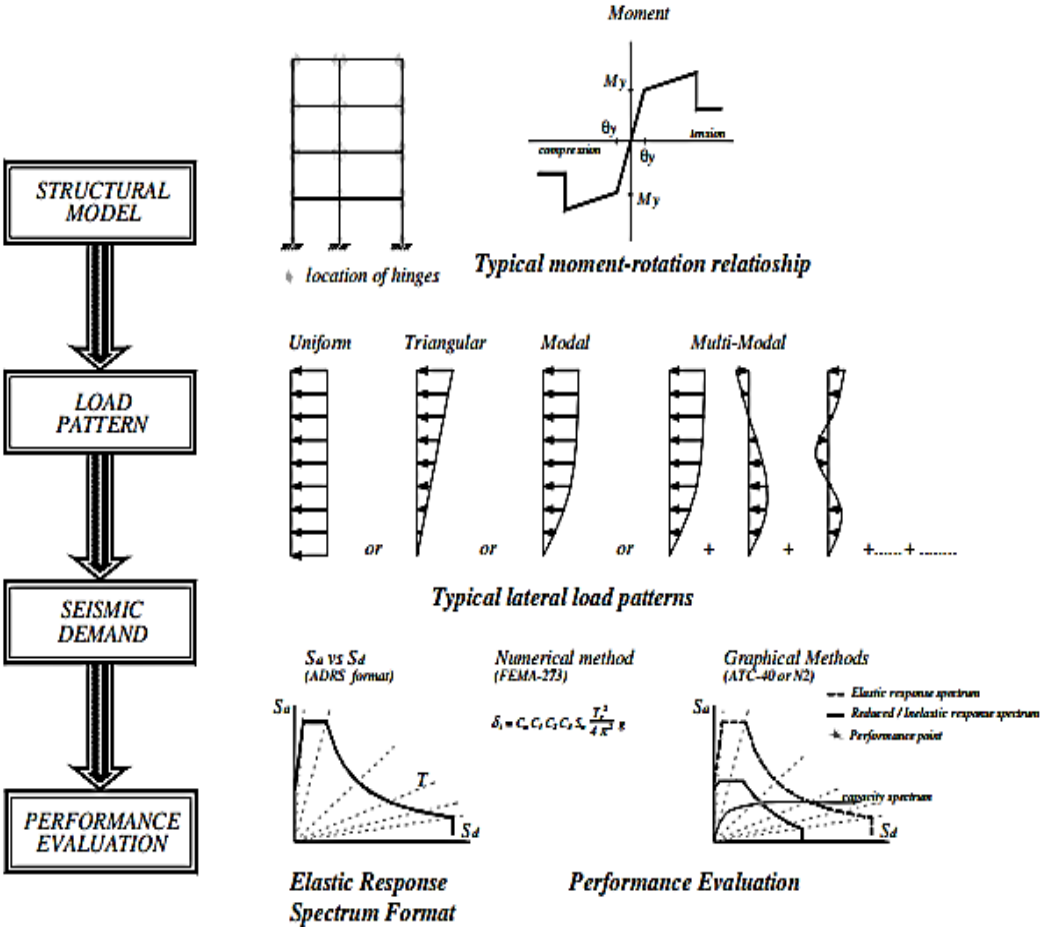

Figure 5: Nonlinear Static Procedure ***[11]***

2.3.1.1 Plastic Hinges

Plastic hinges refer to regions on elements of a structure that undergo plastic deformations during earthquakes or other extreme loads. These domains are expected to undergo severe bending and twisting. They are typically formed in areas such as ending of columns and beams of a frame structure. Plastic hinges are very important in design of structures since allowing some parts of the building to undergo controlled deformation, makes other parts protected by damage [14].

`

If pushover analysis is used properly, it provides very useful information that even time history analysis cannot achieve. One of the most important steps when performing pushover analysis is modelling. During this part, plastic hinges should be carefully located on the elements of the structure [11].

Figure 6 shows Moment-Rotation relationship of a structural element, illustrating the behavior of the element when subjected to both tension and compression. The initial linear points of the curve, from the origin to the yield points, represent the elastic behavior of the material. Beyond these points, the material shows inelastic behavior.

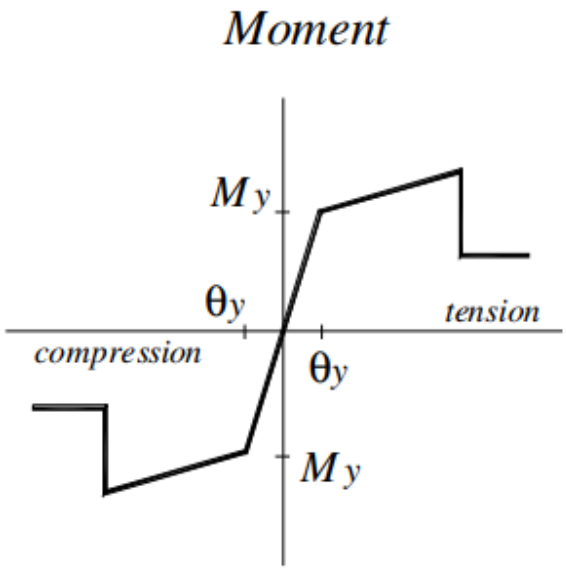

Figure 6: Moment-Rotation relationship ***[11]***

Figure 7 represents the ranges of a typical ductile behaving component. Point A to point B branch represents the elastic range. Point B to point C branch represents plastic range that can include strain hardening or softening. Point C to point E branch shows a strength-degraded range, meaning that the force that should be withstood is less than peak strength [11].

`

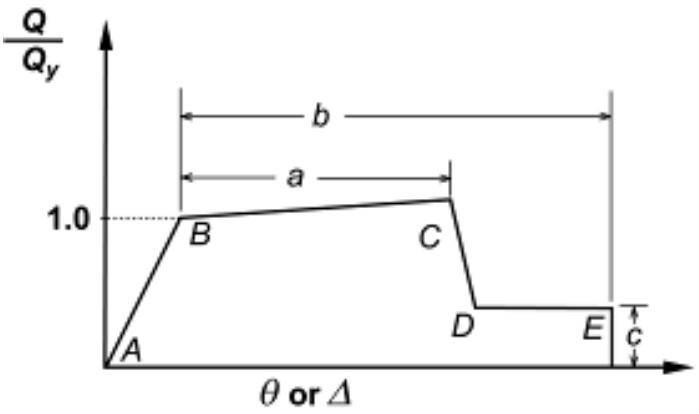

Figure 7: Force-Deformation relation for Concrete Components ***[14]***

Components of the frame such as beams and columns should be designed in a proper way, so that they can represent the inelastic response along their length. For beams and columns, the relationship shown in *Figure 6* shall be plastic hinge rotation or chord rotation. For joints, this relationship shall be shear strain [11].

2.3.1.2 Load Patterns

To achieve the best results, determining the most suitable load pattern is crucial. These patterns should imitate the inertia forces caused by the earthquake to the building. For this reason, sometimes they require selection on higher modes. One single load distribution cannot reflect the alternation of local demands that are expected in a design earthquake. Therefore, at least two load patterns are preferred in non-linear static procedure [9]:

1. Uniform load pattern
2. Modal pattern

One of the disadvantages of using the invariant load pattern for pushover analysis is that it can detect only local mechanisms during an earthquake. None of the lateral load patterns can represent accurately inertia forces since some of the elements of the building may undergo nonlinear behavior [9]. For this reason, adaptive pushover analysis was developed. It starts the analysis with a triangular force distribution. Then this force changes repeatedly during each step of the pushover. This favors the

`

adequate usage of force profiles defined by modal analysis [11]. *Figure 8* shows a schematic representation of load patterns corresponding to higher modes in a structure.

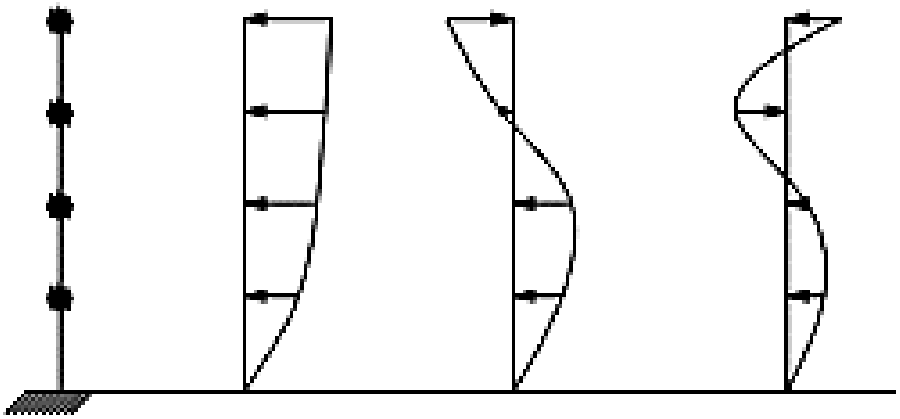

Figure 8: Load patterns corresponding to higher modes ***[11]***

2.3.1.3 Seismic Demand and Performance Evaluation

Seismic demand is seismic threat expressed in ground shaking response spectrum vs accelerogram with or without an estimate of permanent ground deformation [11]. *Figure 9* shows an example of a performance evaluation graph. Key elements shown on this performance evaluation graph are:

1. Response spectrum
2. Capacity Curve
3. Performance Point

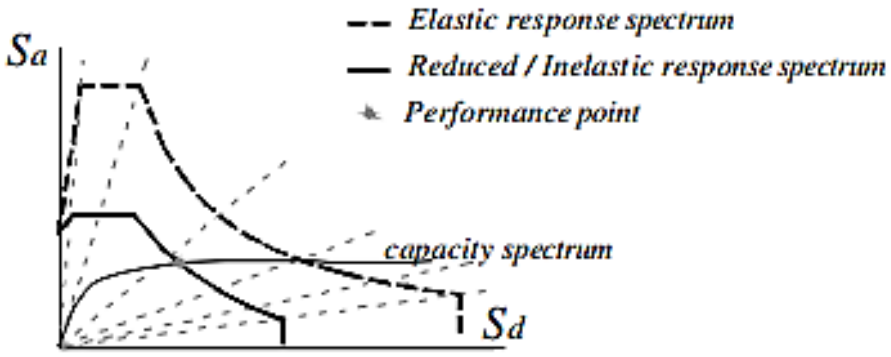

Figure 9: Performance evaluation graph ***[11]***

`

Capacity curve contains each response of the building when it displaces laterally. Deformation for all components of the building reflects global displacement of the structure. This means that each specific point on this curve defines a specific damage state of the structure. By showing on the same graph capacity curve and response spectrum generated by an earthquake motion, their intersection gives the performance point [6]. The performance point estimates the maximum displacement of the building caused by the earthquake. If different performance levels of the capacity curve are compared with this performance point, we can decide whether or not the performance objective is met.

2.3.2 Nonlinear Dynamic Analysis

Time histories of earthquake accelerations are random functions of time. The best way to do the performance assessment of structural systems under seismic loads is through Dynamic Nonlinear Analysis, also known as Time History Analysis. Time History Analysis is a step-by-step procedure which explains the dynamic response of a structure when subjected to seismic loads that vary with time. This analysis is the best method for simulating a structure under extreme ground motion [15]. That is why, in order to perform this analysis, records of previous earthquakes are necessary. Also, it needs a detailed design of the building and to define the viscous damping. Time History Analysis is more time consuming if compared to Pushover Analysis [9].

Time History Analysis procedure is the most accurate one among the methods since it tends to evaluate the building response to real earthquake events. The interpretation of the results from Time History Analysis is complex and requires experience and background knowledge on the field. The results of Time History Analysis are more realistic compared to other methods.

Dynamic response of a structure to arbitrary loading is determined by time history analysis. Dynamic equilibrium equations are given by [5]:

$$\mathrm{K\,u(t) + C\,\dot{u}(t) + M\ddot{u}(t) = r(t)} \qquad \text{(Equation 4)}$$

`

where **K** is stiffness matrix, **C** is damping matrix, **M** is diagonal mass matrix and $\boldsymbol{u}, \dot{\boldsymbol{u}}, and\ \ddot{\boldsymbol{u}}$ are the displacements, velocities and accelerations of the structure, **r** is the applied load. Time histories differ in the type of the load that is applied to the building and also in the type of the analysis that may be performed [8].

2.3.2.1 Incremental Dynamic Analysis

Incremental Dynamic Analysis (IDA) [16] is a comprehensive method used to evaluate the performance of the structures under varying levels of seismic intensity. The approach involves subjecting a structural model to a series of ground motion records, each scaled to different levels of intensity. This generates curves that map the structural response, such as drift or acceleration, against the intensity of the ground motion. These IDA curves provide detailed insights into the structural behavior from elastic through to inelastic and collapse states, allowing for a detailed understanding of how structures will perform under different seismic scenarios.

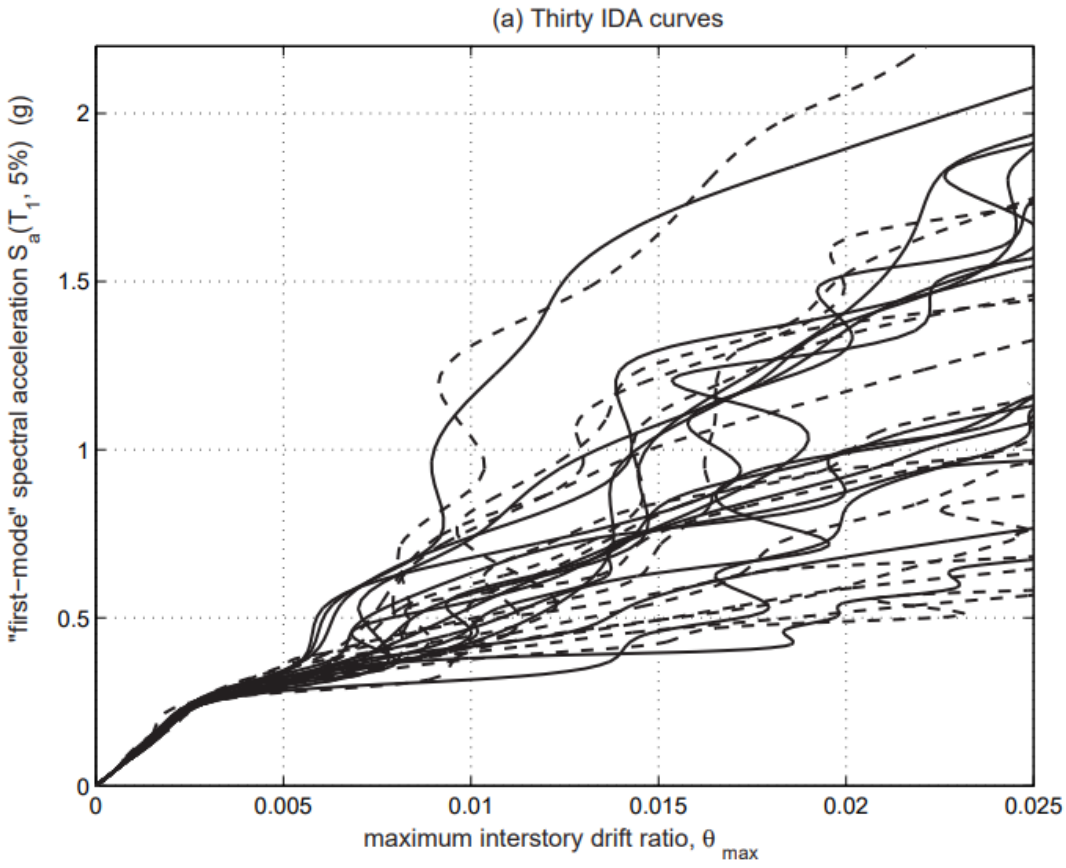

Figure 10: Multi-record IDS curve for a 5-storey building ***[16]***

`

Figure 10 illustrates an example of an IDA study for thirty records on a 5-storey building without shear walls. The IDA methodology is particularly valuable as it highlights the variability in structural response due to different seismic records, enabling a probabilistic assessment of structural performance. By analyzing multiple ground motion records, IDA helps in identifying the range of possible outcomes, which is crucial for performance-based earthquake engineering. The IDA curves are useful for determining the dynamic capacity of structures and understanding the implications of more severe, less frequent ground motions. This method bridges the gap between traditional static pushover analysis and real-world dynamic response [16].

2.4 Pushover Analysis vs. Time History Analysis

According to Özer, Kamal and İnel [17], the comparison of displacement demands from 2D and 3D models showed that 2D models require careful consideration to accurately reflect the behavior of 3D models. Specifically, they found that while 2D nonlinear models can reasonably represent their 3D counterparts, 2D linear elastic models do not adequately capture the complexities of 3D nonlinear behavior.

Pushover Analysis aims to determine capacity of structures in terms of strength and ductility and to identify weak points of the building. After performing Pushover Analysis, we can determine how the building is likely to behave during an earthquake. Pushover Analysis do not account dynamic behavior of earthquakes. As for Time History Analysis, the goal is to understand how the structure will realistically respond to a real earthquake that had happened. It gives a more authentic and complicated assessment of seismic performance.

For small displacement demands, Pushover Analysis and Time History Analysis have similar displacement profiles. However, the displacement pattern from the Pushover Analysis diverges from the predominant mode shape as the earthquake gets stronger. So, Pushover Analysis results may not be always valid. Also, Pushover Analysis may miscalculate the effect of inter-storey drift on buildings [18].

`

For irregular buildings in aspect of geometry, or buildings that have irregular mass or stiffness, it is better to perform a Time History Analysis than Static Pushover Analysis. Either response spectrum method or time history analysis may be used to analyze these buildings [14].

2.5 Computational tools in structural analysis

2.5.1 Overview of software in Structural Engineering

In structural engineering, the use of advanced software has greatly improved how buildings are designed and analyzed. These tools allow engineers to accurately predict how structures will react under different conditions. There are a lot of software available to use in Structural Engineering. SAP2000, ETABS, SAFE etc. are commonly used programs in civil engineering practices.

2.5.2 ETABS Software

ETABS is a powerful program used in civil and structural engineering. It is used by engineers around the world to model, analyze and design building effectively. It has a variety of tools and features and is also simple and easy to use. ETABS offers an integrated set of features for drawing, modeling and analyzing. It has a user-friendly interface and the approach of using the program is straightforward [19].

Using mathematical models, ETABS takes into consideration all the properties of buildings, allowing the computer to represent the model as the real building. When creating, modifying or analyzing a model on ETABS, all the procedure is done through a single interface that is integrated by Microsoft Windows. ETABS offers advanced analytical and design capabilities. This program also provides full static and dynamic analysis [3].

`

2.5.3 NONLIN Software

2.5.3.1 Overview of program features

NONLIN is a program created for being used in structural dynamics and earthquake engineering. It is a user-friendly software, programmed using Microsoft Visual Basic. Both single degree of freedom (SDOF) and multiple degree of freedom (MDOF) models are provided in the software [4].

Load types that are applicable on NONLIN are:

- Periodic loads
- Free Vibration
- Earthquake Loads
- Blast Loading

2.5.3.2 SDOF Model

This is the simplest model provided in NONLIN, and can be described using the following formula [4]:

$$m\ddot{v}(t) + c\dot{v}(t) + R(t) + k_G v(t) = F(t) \qquad (Equation\ 5)$$

Where:

- m is mass system
- c is damping
- R is structural resistance force
- k is initial stiffness
- k_g is geometric stiffness
- F(t) is the applied load as a function of time
- $\ddot{v}$(t) is the computed acceleration
- $\dot{v}$(t) is the computed velocity

`

- v(t) is the computed displacement

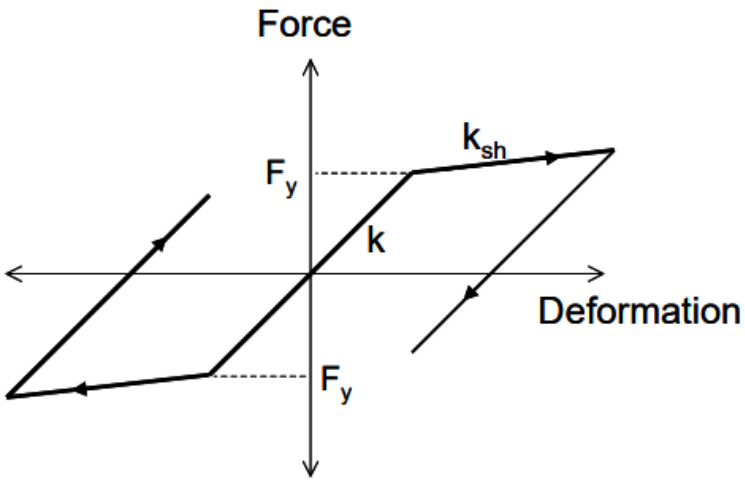

Figure 11: Bilinear Force-Deformation Relationship in SDOF Model ***[4]***

As shown in *Figure 11*, NONLIN used bilinear force-deformation relationship in SDOF models.

`

CHAPTER 3

METHODOLOGY

3.1 Introduction to methodology

The main objective of this study is to evaluate the effectiveness of 2D models compared to their respective 3D model counterparts in predicting response of reinforced concrete buildings to seismic events. The methodology adopted for this study compares the displacement demands from nonlinear time history analyses conducted on both 2D and 3D models. This approach aims to increase the reliability of seismic assessments, which are crucial for safety and stability of infrastructure in earthquake-prone areas.

The methodology section will outline the specific procedures and techniques used to compare 2D and 3D models. This comparison addresses the primary research question regarding the adequacy of 2D models in reflecting 3D models. It also contributes to broader engineering practices validating simpler modeling approaches when studying seismic events' effects on structures.

3.2 Pushover Analysis using ETABS

Pushover analysis is a nonlinear static analysis method used to estimate the seismic capacity of a structure [13]. The following steps outline the procedure for conducting pushover analysis using ETABS:

1. Preparation of Structural Model
2. Defining Pushover Load Patterns
3. Assigning Pushover Hinges
4. Performing Pushover Analysis
5. Obtaining Capacity Curves

`

3.2.1 Plastic Hinges Installation

The pushover analysis procedure begins with preparation of the structural models on ETABS. Models were defined with precise material characteristics and geometrical properties. Plastic hinges play a significant role in pushover analysis results. Equation 6 expresses the relationship of plastic hinge length and the length of the element that the hinge is assigned, where L_p is the length of the plastic hinge and $H_{b/c}$ is the length of the element, beam or column [14].

$$L_p = 0.1 * H_{b/c} \qquad (Equation\ 6)$$

3.2.2 Load Application

Gravitational loads, including dead and live loads reflect the loads coming from the slabs. Mass source defines how the mass is calculated for seismic analysis. For this study, loads considered on mass source are dead loads and live loads. Dead loads include loads coming from the slabs, beams and columns and live loads are variable loads added on each beam. Dead load multiplier on mass source is 1 while live load multiplier is 0.3. This means that 100% of dead load of the structure contributes on mass source. Since live loads are loads that can vary in magnitude and location only 30% of their magnitude is considered as mass source [9].

While performing pushover analysis on ETABS, these different types of load cases were applied to understand how the structure reacts under seismic events. The first load case to be considered is Gravity Load. Gravity Load refers to loads that are due to gravitational force acting on the structure. This includes both dead and live loads.

Modal Load refers to loads derived from modal analysis. It is not a direct load type like gravity that includes dead and live loads and it is used to identify the natural frequencies of mode shapes of a structure. Multi-degree of freedom systems have multi modes of vibration. The highest mode is the natural period of the building. Natural period magnitude is approximately equal to:

$$T = 0.1 * H$$

`

Where:

- T is the natural period in seconds
- H is the total height of the building in meters

The capacity curve obtained by ETABS is Base Shear vs. Top Roof Displacement. Using Microsoft Excel, the graph was converted into Base Shear/ Seismic Weight vs. Roof Drift (%). Base Shear is divided with total weight of the building and Top Roof Displacement is divided with total height of the building.

3.3 Bilinearization of Capacity Curves

The first step before proceeding with Time History is bilinearization of the structure. Bilinearization simplifies the representation of the structure. This process converts multi-degree-of-freedom (MDOF) systems into simpler single-degree-of-freedom (SDOF) systems. NONLIN software that is used in this study to perform time history analyses, operates with SDOF systems. [4] *Figure 11* shows bilinearization of pushover curve, where the bold line is the pushover curve (real curve) and the dashed line is the bi-linearized curve (idealized curve).

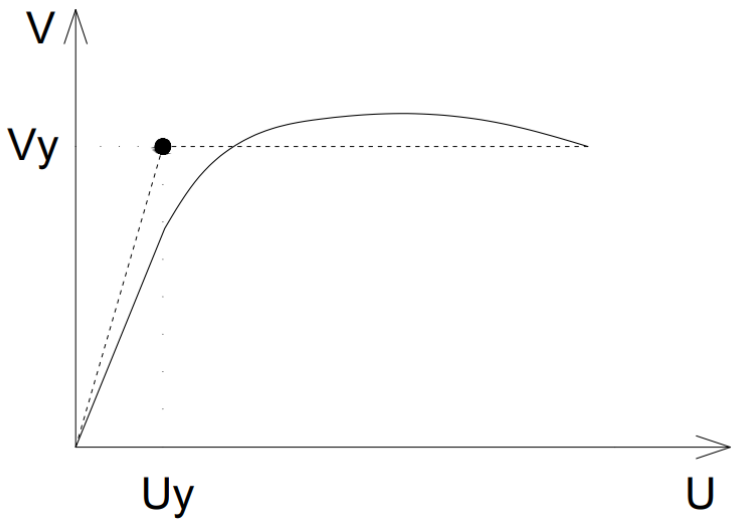

Figure 12: Pushover Curve Bilinearization ***[20]***

`

As shown in *Figure 12*, the bi-linearized curve consists of two linear branches. According to this method, the idealized curve starts with a linear function going with a specified slope k_1, and finishes with another linear function with a different slope k_2. The second branch of the idealized curve goes till approximately 85% of the maximum base shear. The goal of bilinearization process is reached when the areas between idealized curve and real pushover curve are equal [20]. *Equation 7* [20] and *Equation 8* [20] represent the stiffness of the first linear branch in the idealized curve and the positive yield strength normalized by modal mass coefficient respectively.

$$k_1 = \frac{V_y}{d_y} \qquad (Equation\ 7)$$

$$\sigma = \frac{V_y}{\alpha} \qquad (Equation\ 8)$$

$$\alpha_1 = \frac{\left[\sum_{i=1}^{N} \frac{w_i \phi_{i1}}{g}\right]^2}{\left[\sum_{i=1}^{N} \frac{w_i}{g}\right]\left[\sum_{i=0}^{N} \frac{w_i \phi_{i1}^2}{g}\right]} \qquad (Equation\ 9)$$

Where:

- k_1 is stiffness of the first linear branch in the idealized curve
- k_2 is stiffness of the second horizontal branch in the idealized curve
- σ is positive yield strength
- α is modal mass coefficient for the first natural mode
- $\frac{w_i}{g}$ is the mass assigned to level i
- ϕ_{i1} is the amplitude of mode 1 at level i
- N is the highest storey level of the structure

`

3.4 Nonlinear Time History Analysis using NONLIN

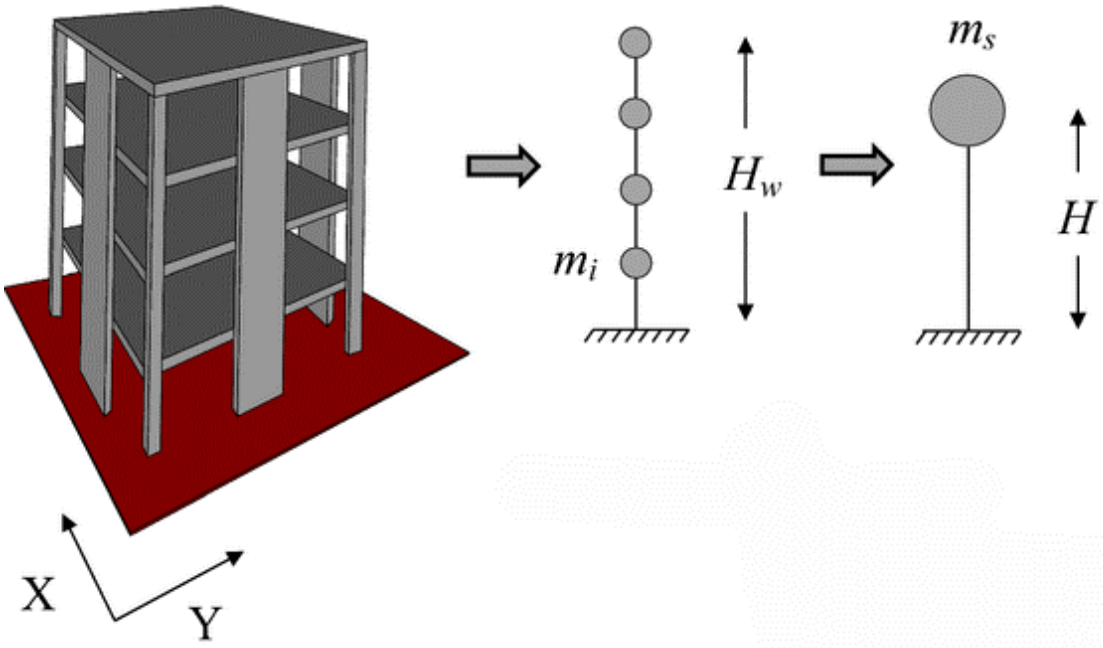

Figure 13: Transformation of MDOF to SDOF ***[22]***

Figure 13 shows the transformation of multi-degree-of-freedom system (MDOF) to single-degree-of-freedom system (SDOF). FEMA-356 [23], explains how to convert MDOF systems to equivalent SDOF systems.

Parameters needed to perform time history analysis in order to obtain displacement demand in NONLIN are W, c, k_1, k_2 and σ, where:

- W is the total weight of the structure in kN
- c is the structural damping in %
- k_1 is the structural stiffness in kN/m
- k_2 is the structural strain hardening stiffness in kN/m
- σ is structural yield strength in kN

`

Before entering these values in NONLIN, a few calculations should be previously made for calculating k_1, k_2 and σ as previously explained in *Equation 7*, *Equation 8* and *Equation 9*. *Figure 14* illustrates the key input parameters of performing nonlinear dynamic analysis in NONLIN.

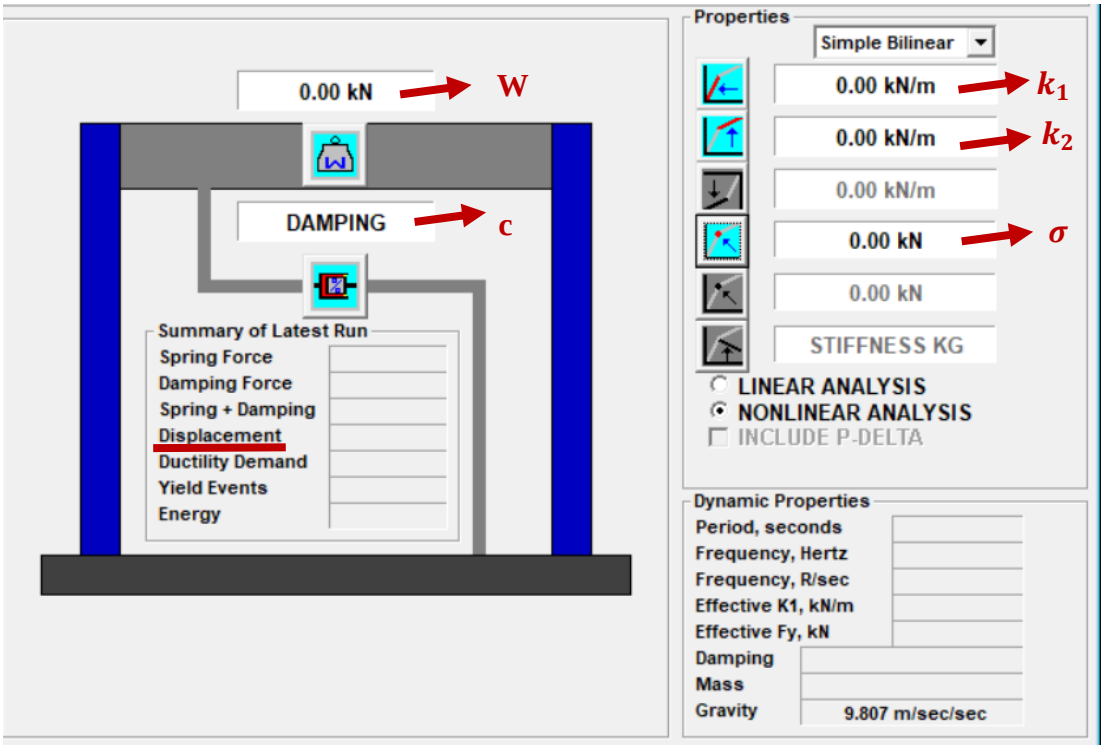

Figure 14: Input parameters for nonlinear analysis in NONLIN

The next step is to input the earthquake records that are included in the database of NONLIN. The output taken from the analyses is the displacement.

The displacement taken from these analyses in NONILN are for SDOF systems, which simplifies the analysis by assuming a single point of displacement. [4] However, the buildings considered for this study are represented as MDOF systems. It is necessary to convert SDOF displacement to MDOF displacement. This conversion is done by multiplying the displacement taken from Nonlin with PF_1, which is calculated as shown in *Equation 10* [21]:

$$PF_1 = \left[\frac{\sum_{i=1}^{N} \frac{w_i \phi_{i1}}{g}}{\sum_{i=0}^{N} \frac{w_i \phi_{i1}^2}{g}}\right] \qquad (Equation\ 10)$$

`

Where:

- PF_1 is the modal participation factor for the first natural mode
- $\frac{w_i}{g}$ is the mass assigned to level i
- ϕ_{i1} is the amplitude of mode 1 at level i
- N is the highest storey level of the structure [21]

`

CHAPTER 4

CASE STUDY

ETABS and Nonlin software were used for running nonlinear static and dynamic analyses. ETABS is a widely recognized structural analysis and design software, that is capable of handling complex structural modeling and is accepted in both academic and professional circles for earthquake engineering studies. [19] Modelling of three buildings together with the selected 2D frames and nonlinear static analyses were performed using ETABS software. Nonlinear dynamic analyses were conducted using Nonlin software, specialized for dynamic simulation and offering precise control over nonlinearity effects in structures [4].

4.1 Description of Building Models

For this study, three typical reinforced concrete buildings without shear walls were selected in order to perform both nonlinear static and dynamic analyses. These buildings were selected to represent low to mid-rise reinforced concrete buildings, located in high seismic zones of Albania. Three buildings share the same plan, but differ in the number of stories. They consist of 5, 8 and 12 stories respectively. The variation in building heights allows the comparison of seismic analyses results. The buildings are regular and the plan is symmetrical in both principal directions.

As show in *Figure 15*, the plan view of the buildings consists of four spans in both x- and y-directions. In x-direction each span is 4.5 m and in y-direction each span is 3.5 m. The height of each floor is 3 m, making the buildings 15 m, 24 m and 36 m high respectively. The buildings differ not only in elevation, but also in beam and column cross-sections, concrete and steel grades and longitudinal and transverse reinforcement.

`

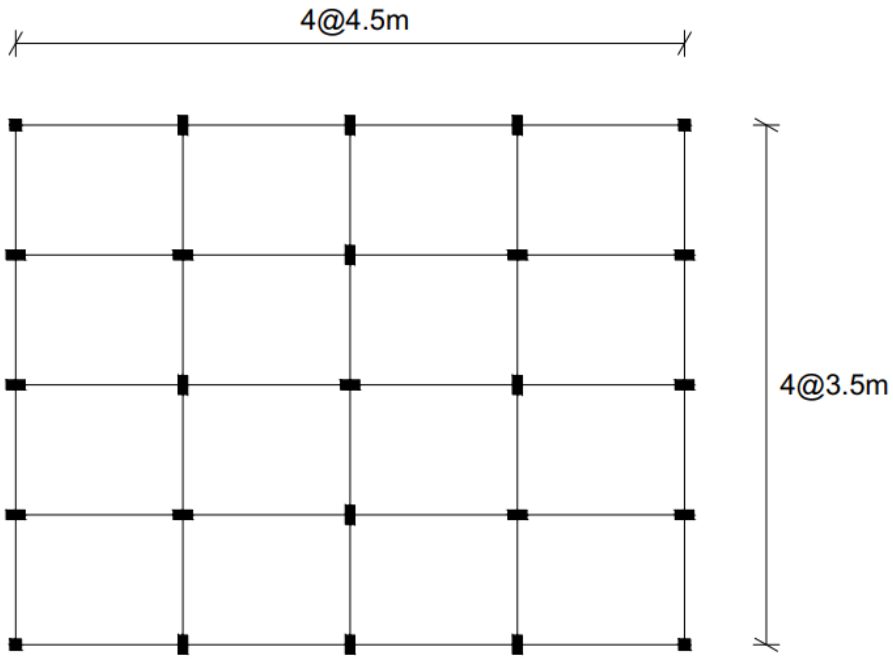

Figure 15: Plan view of 5-, 8-, and 12-storey building ***[24]***

The 5-storey building consist of 250x500 mm inner columns, 300x300 mm corner columns and 200x500 mm beams. All these elements are modelled using C16/20 concrete. The 8-storey building consist of 300x600 mm inner columns, 400x400 mm corner columns and 250x600 mm beams. Both beams and columns are modelled using C20/25 concrete. The 12-storey building consist of 350x700 mm inner columns, 650x650 mm corner columns ad 300x650 mm beams. All elements are modelled using C30/37 concrete. Yield strength of steel for all cases in both longitudinal and transverse reinforcement is 220 MPa, while concrete compressive strength differs for each building. Amount of longitudinal steel of the beams is considered as 1.2% of the beam cross-sectional area. [24]. All the characteristics of the buildings are summarized in *Table 2*:

`

Table 2: Key characteristics of buildings modeled in ETABS

	5-Storey Building	**8-Storey Building**	**12-Storey Building**
Concrete Grade	C16/20	C20/25	C30/37
Steel Yield Strength	S220	S220	S220
Inner Column Dimensions [mm]	250x500	300x600	350x700
Corner Columns Dimensions [mm]	300x300	400x400	650x650
Beam Dimensions [mm]	200x500	250x600	300x650

Both longitudinal and transverse reinforcement have $f_{yk} = 220\ MPa$, $f_{su} = 340\ MPa$ and $\epsilon_{su} = 0.18$, where:

- f_{yk} is characteristic yield strength of the reinforcing steel
- f_{su} is the ultimate strength of steel
- ϵ_{su} is ultimate strain of steel

Transverse reinforcement is considered 10 mm diameter with 100 mm spacing in all cases. *Figure 16* illustrates column cross-sections of corner and inner columns of the three building models.

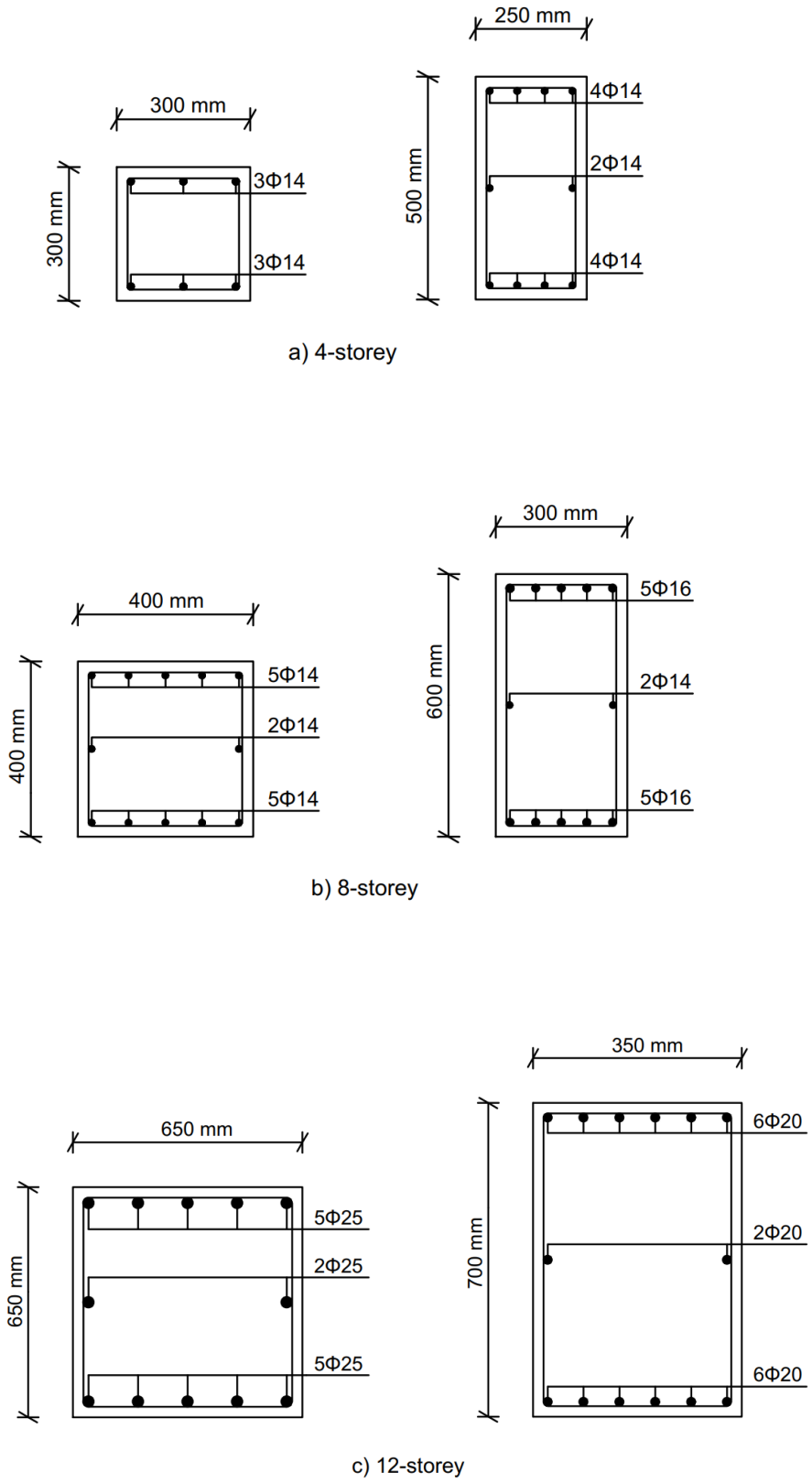

Figure 16: Corner (left) and inner (right) column cross-sections for 5-, 8- and 12-storey buildings ***[24]***

`

4.2 Development of 2D and 3D models

In this study, analyzing the seismic response involves both two-dimensional (2D) models and three-dimensional (3D) models of the three low-to-mid-rise reinforced concrete buildings selected. Firstly, 3D models were carefully created on ETABS, followed by the derivation of 2D model frames from their respective 3D models.

4.2.1 3D Modeling

The 3D models reflect the actual geometry of the building, making the modeled and real buildings as similar as possible. The buildings consist of beams and columns. For this study, the buildings do not incorporate shear walls, making the buildings rely only on beams and columns for seismic response.

Firstly, the material properties such as type of concrete and steel were defined as shown in *Table 2*. Then, each cross-section of every element of the frame was carefully modeled as shown in *Figure 16*, using the respective material and dimensions for each building. The frame elements were drawn based on the floor plan and storey elevation. The supports at the base of the buildings were considered fixed.

As observed from the floor plan on *Figure 15*, the building consists of 16 slabs with the same dimensions. According to *Equation 3*, these slabs are all two-way slabs.

$$\frac{l_x}{l_y} > 2 \quad One - Way\ Salb \qquad (Equation\ 11)$$

$$\frac{l_x}{l_y} \leq 2 \quad Two - Way\ Salb \qquad (Equation\ 12)$$

Where:

- l_x is the largest dimension of the slab
- l_y is the smallest dimension of the slab

`

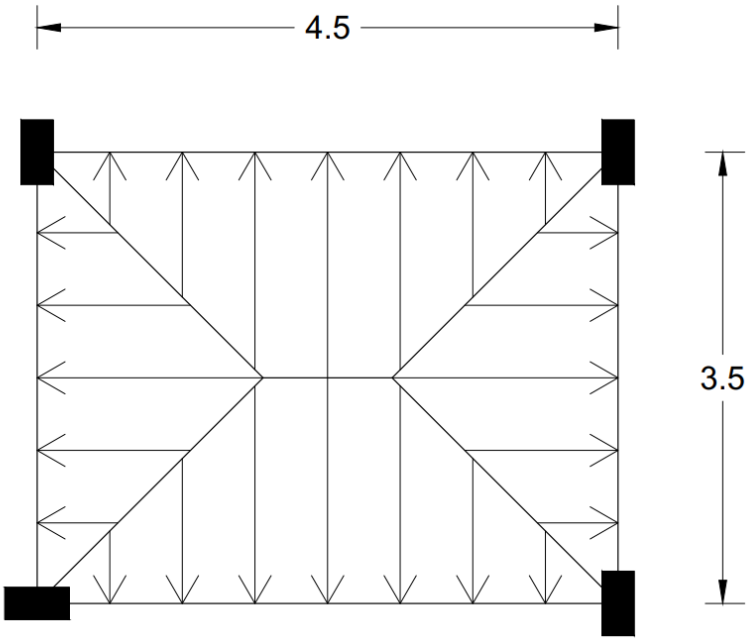

Figure 17: Load distribution on two-way slabs of selected buildings ***[24]***

$$\frac{l_x}{l_y} = \frac{4.5\ m}{3.5\ m} = 1.28 < 2 \qquad Two - way\ slab$$

Figure 17 shows load distribution on each slab. In this study, both dead and live loads were calculated and added to the beams of each slab. Since they were all two-way slabs, the loads were added as trapezoidal and triangular shaped based on the beam length. Dead loads were applied on each beam of the buildings, while live loads were applied to the beams of all stories except the top story, where no live load is anticipated.

$$G_k = \gamma_C * t_s \qquad (Equation\ 13)$$

Where:

- G_k is the permanent load
- γ_C is the concrete unit weight
- t_S is the slab thickness

$$G_k = \gamma_C * t_s = 25\frac{kN}{m^3} * 0.2\ m = 5\frac{kN}{m^2}$$

`

$$Q_k = 2\frac{kN}{m^2}$$

Where:

- Q_k is the variable load

Floor diaphragms are assumed to be rigid in its plane, allowing the appropriate distribution of lateral forces and moments within the structure during seismic events. On ETABS they were implemented as rigid separately on each floor for each building.

4.3.2 2D Modeling

2D models are simplified versions of the real buildings, as shown in *Figure 18*. They are extracted from the critical frames of 3D models on two orthogonal directions. They consist of beams and columns that have the same geometrical and material properties as 3D models. This approach helps in understanding how well the response of critical models will reflect the response of 3D models during seismic events.

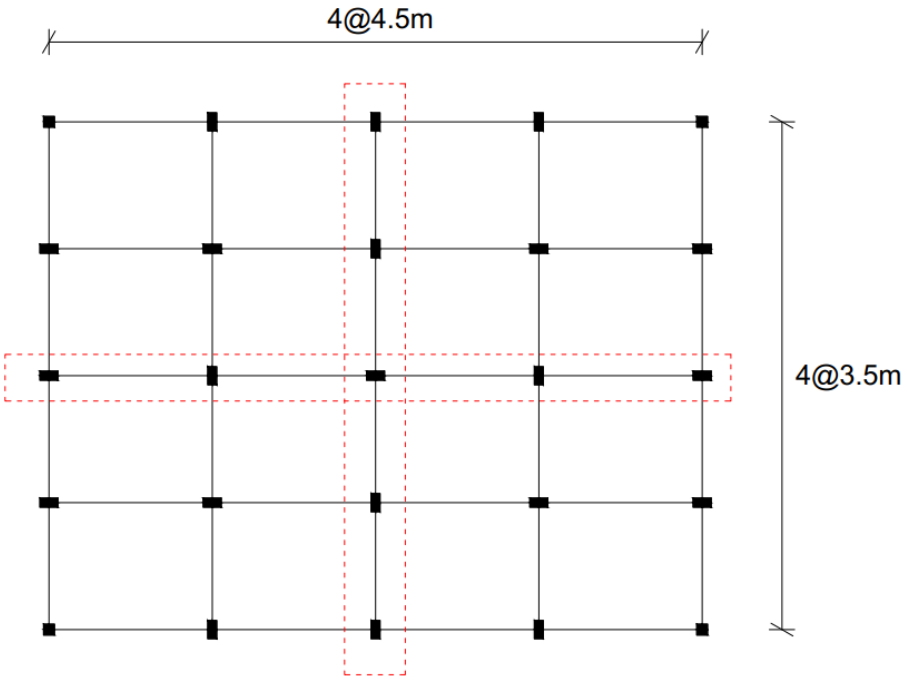

Figure 18: The selected 2D frames ***[24]***

`

4.3 Pushover Analysis Procedure

4.3.1 Plastic Hinges Installation

The pushover analysis procedure begins with preparation of the structural models on ETABS. Models were defined with precise material characteristics and geometrical properties. Plastic hinges play a significant role in pushover analysis results. For this study, the distances of plastic hinges were considered as 10% of the clear length of the element from both supports, on both beams and columns. P-M2-M3 hinge property was used for columns and M3 hinge property was used for beams. *Figure 19* represents the hinges assigned on each element of the frame.

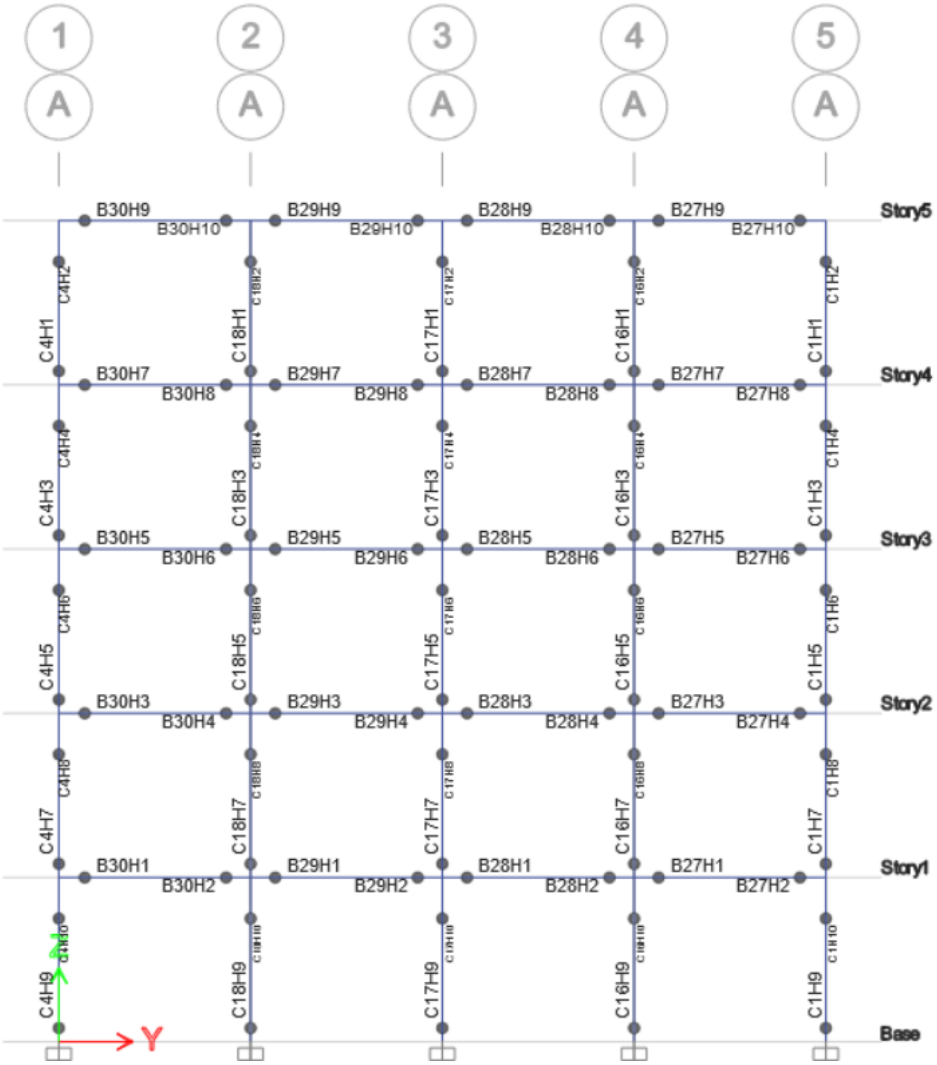

Figure 19: Plastic hinges assigned on ETABS

`

4.3.2 Load Application

Load cases used for this study which are also shown in *Figure 20* for performing pushover analysis are:

- Gravity
- Modal
- Pushover in X direction
- Pushover in Y direction

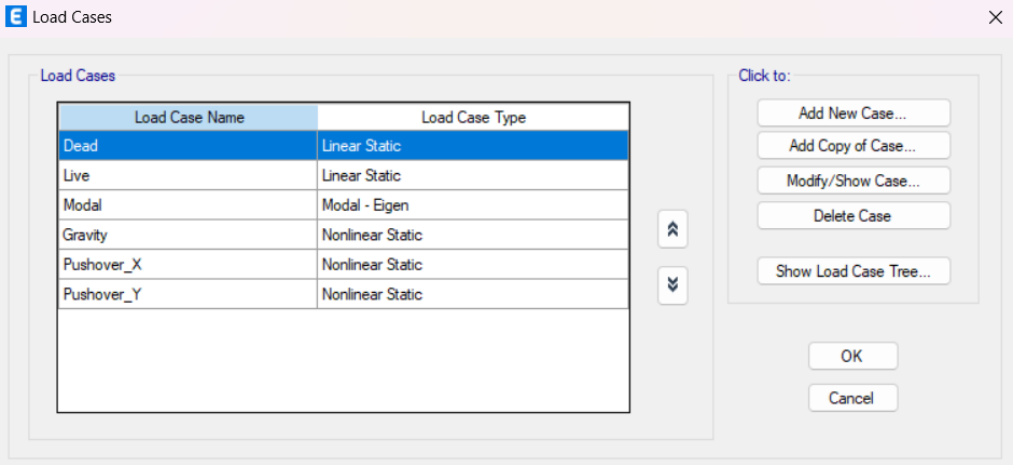

Figure 20: Load Cases used for performing the analyses

While performing pushover analysis on ETABS, these different types of load cases were applied to understand how the structure reacts under seismic events. The first load case to be considered was Gravity Load. Gravity Load refers to loads that are due to gravitational force acting on the structure. This includes both dead and live loads.

Modal Load refers to loads derived from modal analysis. It is not a direct load type like gravity that includes dead and live loads and it is used to identify the natural frequencies of mode shapes of a structure. In *Table 3*, *Table 4* and *Table 5*, natural period in seconds and total weight in kN of each model modelled on ETABS are shown. These values were taken directly from the program.

`

Table 3: 5-Sorey Building, Periods and Weights in X and Y directions

5-STOREY BUILDING		
	Period (s)	**Weight (kN)**
3D-5S-X	0.66	7843.454
3D-5S-Y	0.646	7843.454
2D-5S-X	0.56	1181.144
2D-5S-Y	0.4	868.6281

Table 4: 8-Sorey Building, Periods and Weights in X and Y directions

8-STOREY BUILDING		
	Period (s)	**Weight (kN)**
3D-5S-X	0.838	18588.2
3D-5S-Y	0.826	18588.2
2D-5S-X	0.72	2781.381
2D-5S-Y	0.53	1988.946

Table 5: 12-Sorey Building, Periods and Weights in X and Y directions

12-STOREY BUILDING		
	Period (s)	**Weight (kN)**
3D-5S-X	1.21	28916.33
3D-5S-Y	1.15	28916.33
2D-5S-X	1.06	4341.6
2D-5S-Y	0.82	3259.2

As observed from the above tables, *Equation 14* is satisfied in most cases except Y direction in 2D models. This is due to the fact that the beams of the critical frames in Y direction withstand less load from the slabs. This is reflected in values of periods. The smaller the mass, the smaller the period and vice versa [5].

$$T = 2\pi * \sqrt{\frac{m}{k}} \qquad (Equation\ 14)$$

`

Where:

- T is the natural period in seconds [s]
- m is the total mass of the building in kilograms [kg]
- k is the stiffness in newtons per meter [N/m]

4.3.3 Analysis Execution

The next step after defining load cases was running the analysis. This process was repeated for the three buildings. From the modal analysis the period of the building in the first two modes was obtained. The output taken from pushover analysis was the capacity curve. Firstly, the 3D building models were analyzed, followed by six 2D models. So, a total of twelve capacity curves were obtained by ETABS. Capacity curves obtained from pushover analysis have roof displacement on x-axis and base shear on y-axis. All these values were exported on an Excel sheet for further calculations.

From the modal load case it was concluded that the 5-storey building has a 0.66 s period in x-direction and 0.65 s period in y-direction. This helps in conducting pushover analysis in x- and y- directions, since it applies a distribution of loads that is proportional with the mode shapes of the building. Load application is displacement controlled. 4% of the height of the building is said to be the target displacement. The target displacement is the maximum estimated displacement that the building experiences during an earthquake. For example, the height of the 5-storey building is 15 m, the target displacement is 600 mm. Total weight of 5-storey building is 7843.45 kN. Figure 21 illustrates the capacity curve as obtained from ETABS, with Roof Displacement in mm on x-axis and Base Shear in kN on y-axis. Figure 22 shows the normalized version of the capacity curve, with Roof Drift in % on x-axis and Base Shear normalized with the Seismic Weight on y-axis.

`

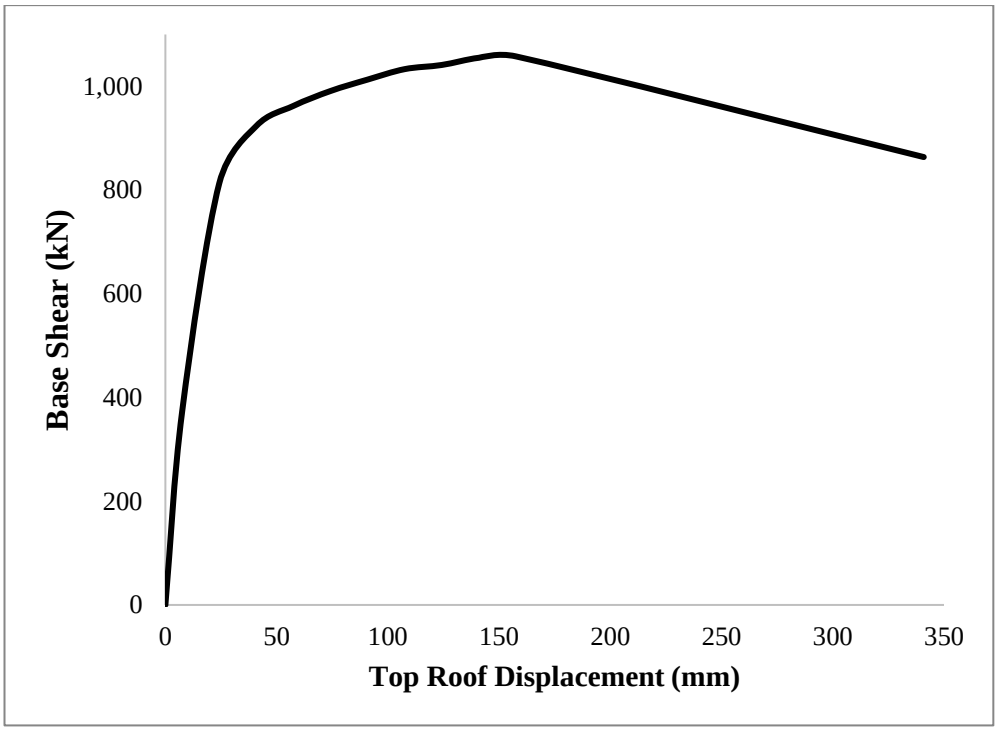

Figure 21: Base Shear vs. Roof Displacement

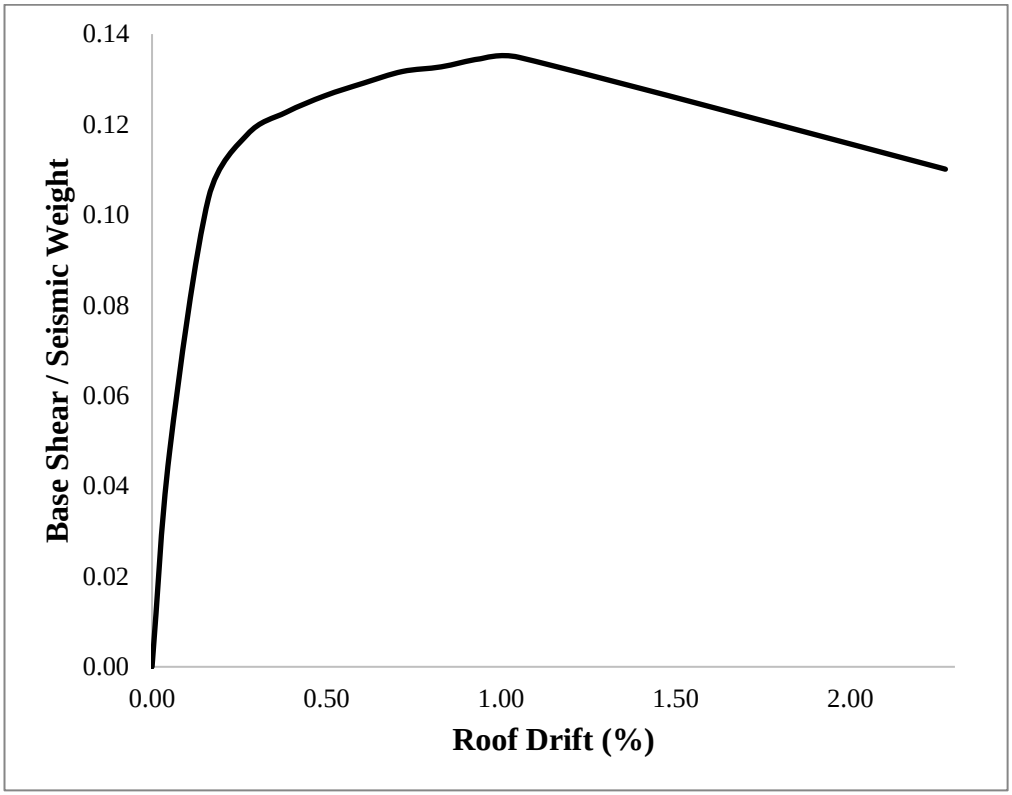

Figure 22: Base Shear / Seismic Weight vs. Roof Drift Curve

`

4.4 Time History Analyses Procedure

4.4.1 Bilinearization Process

Figure 23 shows bilinearization process of 3D 5-steorey building. In this example, direction x of the pushover is considered. The first step of bilinearization is to simplify the pushover curve. For this an energy equivalent analysis is used. During equivalent energy analysis, areas are compared in order to reach the results.

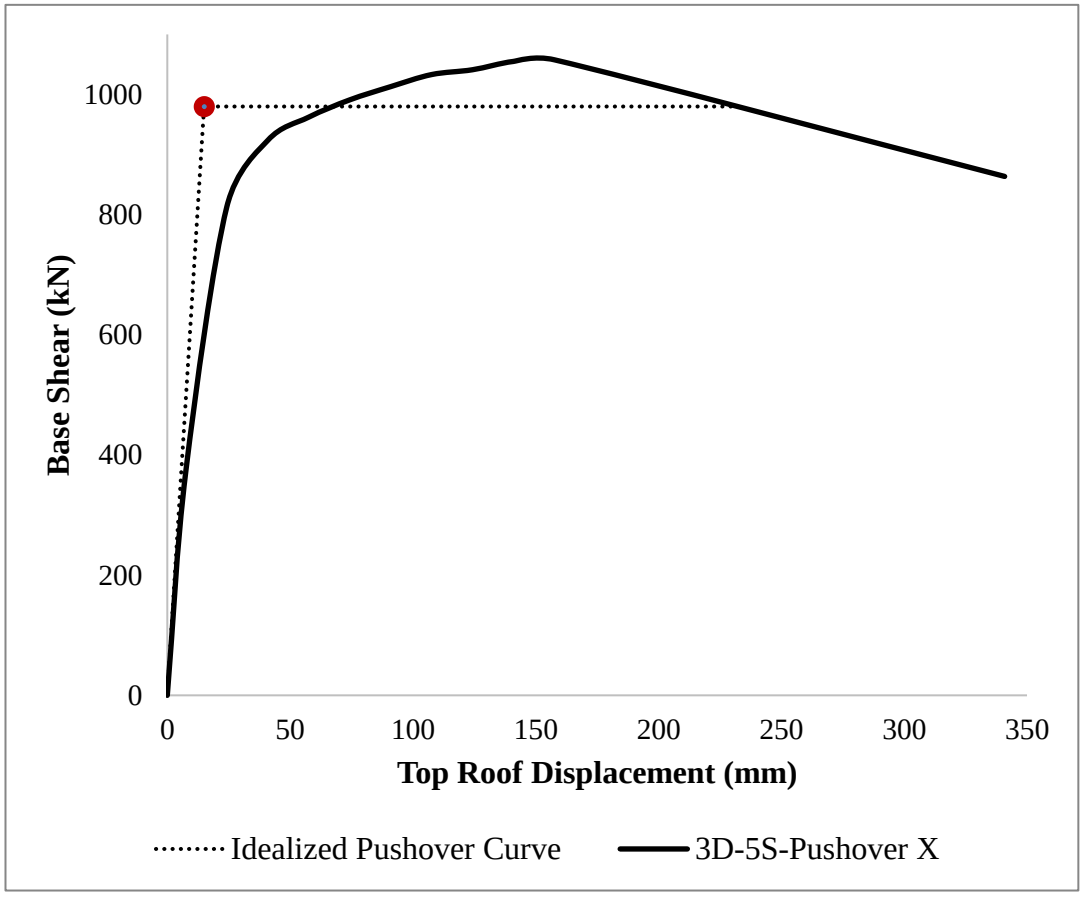

Figure 23: Bilinearization of Pushover Curve 3D 5-Storey Building (X-Direction)

When the areas under both the real and the idealized pushover curve are equal, as shown in *Figure 23*, the following values showed in *Table 6* are gathered in order to proceed with time history analyses:

`

Table 6: Parameters used for Time History Analysis

Parameter	Unit	
dy	[kN]	0.02
Vy	[kN]	980.00
W	[kN]	7843.50
c	[%]	5.00
α	-	0.85

Where:

- V_y is base shear force at yield
- d_y is corresponding lateral displacement at yield
- W is total weight of the building
- c is structural damping
- α is modal mass coefficient for the first natural mode

After obtaining these parameters, a few calculations following the procedure as shown in methodology part, are done in order to find the required data for running Nonlin software. *Table 7* shows the results of these calculations.

$$k_1 = \frac{V_y}{d_y}$$

$$k_2 = 0$$

$$\sigma = \frac{V_y}{\alpha}$$

Table 7: Parameters used for Time History Analysis

Parameter	Unit	
k1	[kN/m]	65333.33
k2	[kN/m]	0.00
σ	[kN]	1152.94

`

4.4.2 Nonlinear Time History Analyses

Parameters used to run Nonlin software are k1, k2, σ, W and c. After these parameters were calculated, one of 146 earthquake records provided in the software were selected. From these 146 records, 68 of them are far-field records and 78 are near-field records. A total of three 3D buildings and six 2D buildings were analyzed in ETABS, resulting in 12 pushover curves. For each pushover curve the bilinearization process was followed and all the above parameters were calculated. These values were inputted in NONLIN software to perform time history analysis. A total of 1752 time history analyses were performed in Nonlin. The output taken from the software is the displacement, which will be used in order to compare the displacement demand of 2D and 3D models.

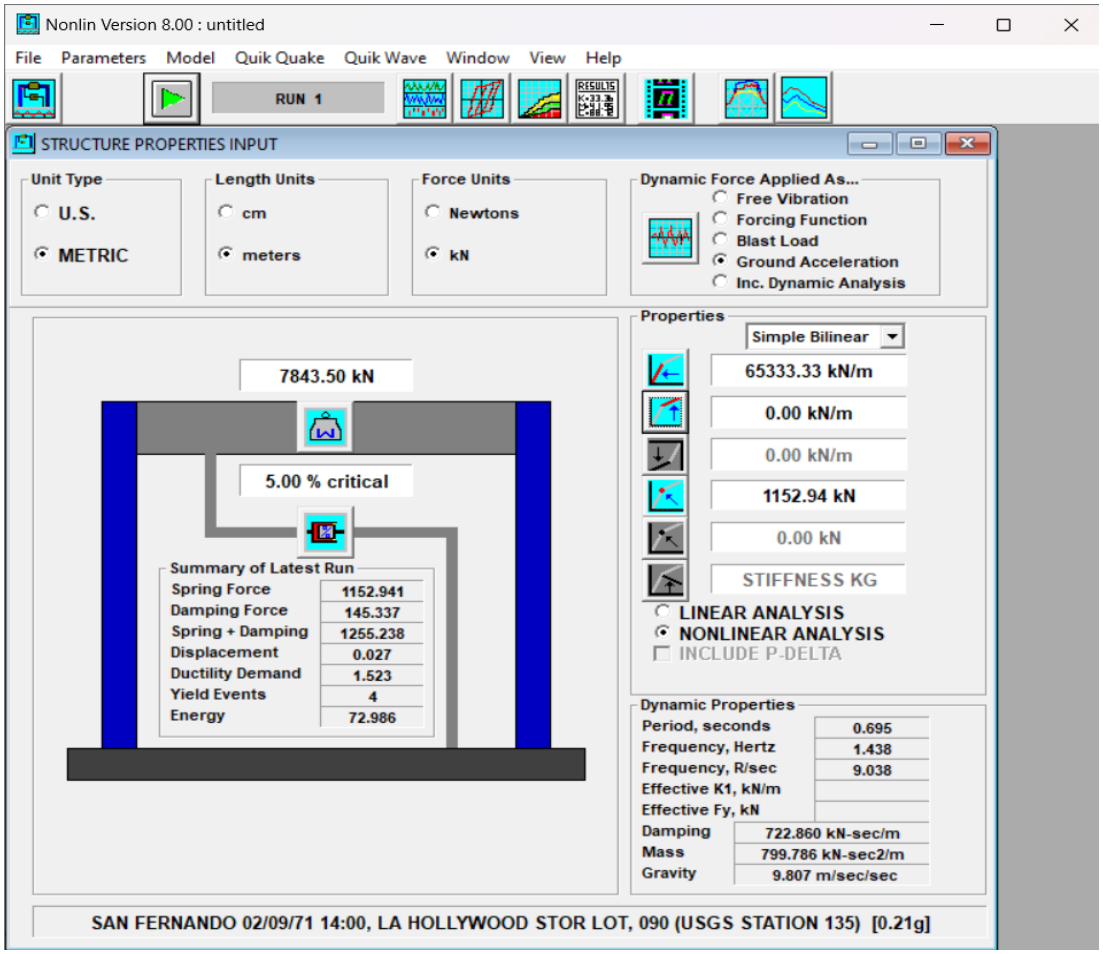

Figure 24: Running the analysis in NONLIN

`

The value of displacement is taken from Nonlin. This value shows the displacement for SDOF system, while in reality the buildings are MDOF systems. The value of displacement taken for each earthquake is multiplied with modal participation factor, calculated with the following formula:

$$PF_1 = \left[\frac{\sum_{i=1}^{N} \frac{w_i \phi_{i1}}{g}}{\sum_{i=0}^{N} \frac{w_i \phi_{i1}^2}{g}}\right]$$

After multiplying the value of displacement with PF_1, the obtained values were normalized with the height of recpective building and turned into percentage. Normalizing the values helps in comparing and analyzing the data.

Table 8: Far-Field Records, Roof Drift Demands of 3D 5-, 8-, 12-storey building models (%)

			3D					
			5-Storey		8-Storey		12-Storey	
	Earthquake	**Type**	**X**	**Y**	**X**	**Y**	**X**	**Y**
1	SanFernando_LA_HollywoodStor_90	Far Field	0.23	0.23	0.33	0.31	0.20	0.21
2	SanFernando_LA_HollywoodStor_180	Far Field	0.18	0.18	0.14	0.16	0.11	0.12
3	SanFernando_LA_HollywoodStor_V	Far Field	0.06	0.06	0.07	0.06	0.06	0.06
4	Friuli-Italy-Tolmezzo_00	Far Field	0.29	0.29	0.29	0.27	0.25	0.26
5	Friuli-Italy-Tolmezzo_270	Far Field	0.64	0.63	0.40	0.39	0.20	0.20
6	Friuli-Italy-Tolmezzo_V	Far Field	0.09	0.09	0.07	0.09	0.06	0.06
7	ImperialValley-06_Delta_262	Far Field	0.76	0.75	0.40	0.41	0.27	0.27
8	ImperialValley-06_Delta_352	Far Field	0.75	0.75	0.45	0.47	0.41	0.43
9	ImperialValley-06_Delta_V	Far Field	0.11	0.11	0.07	0.07	0.10	0.10
10	ImperialValley-06_Delta_ElCentro11_140	Far Field	0.57	0.57	0.28	0.27	0.44	0.45
11	ImperialValley-06_Delta_ElCentro11_230	Far Field	0.37	0.37	0.26	0.26	0.50	0.50
12	ImperialValley-06_Delta_ElCentro11_V	Far Field	0.06	0.06	0.06	0.07	0.05	0.05
13	SuperstitionHills02_ElCentromp_00	Far Field	1.00	0.99	0.51	0.53	0.41	0.42
14	SuperstitionHills02_ElCentromp_90	Far Field	0.34	0.34	0.16	0.17	0.36	0.36
15	SuperstitionHills02_ElCentromp_V	Far Field	0.13	0.13	0.13	0.13	0.08	0.08

`

Table 9: Far-Field Records, Roof Drift Demands of 2D 5-, 8-, 12-storey building models (%)

			2D					
			5-Storey		8-Storey		12-Storey	
	Earthquake	**Type**	**X**	**Y**	**X**	**Y**	**X**	**Y**
1	SanFernando_LA_HollywoodStor_90	Far Field	0.25	0.25	0.19	0.15	0.35	0.10
2	SanFernando_LA_HollywoodStor_180	Far Field	0.16	0.16	0.11	0.10	0.13	0.06
3	SanFernando_LA_HollywoodStor_V	Far Field	0.05	0.05	0.05	0.03	0.12	0.02
4	Friuli-Italy-Tolmezzo_00	Far Field	0.30	0.30	0.28	0.19	0.28	0.11
5	Friuli-Italy-Tolmezzo_270	Far Field	0.54	0.54	0.46	0.49	0.22	0.23
6	Friuli-Italy-Tolmezzo_V	Far Field	0.08	0.08	0.06	0.05	0.07	0.04
7	ImperialValley-06_Delta_262	Far Field	0.27	0.27	0.43	0.24	0.26	0.17
8	ImperialValley-06_Delta_352	Far Field	0.40	0.40	0.36	0.40	0.43	0.17
9	ImperialValley-06_Delta_V	Far Field	0.08	0.08	0.09	0.05	0.11	0.04
10	ImperialValley-06_Delta_ElCentro11_140	Far Field	0.34	0.34	0.29	0.21	0.37	0.17
11	ImperialValley-06_Delta_ElCentro11_230	Far Field	0.27	0.27	0.39	0.28	0.34	0.19
12	ImperialValley-06_Delta_ElCentro11_V	Far Field	0.05	0.05	0.04	0.03	0.04	0.02
13	SuperstitionHills02_ElCentromp_00	Far Field	0.69	0.69	0.46	0.34	0.45	0.19
14	SuperstitionHills02_ElCentromp_90	Far Field	0.33	0.33	0.16	0.16	0.53	0.10
15	SuperstitionHills02_ElCentromp_V	Far Field	0.08	0.08	0.08	0.08	0.13	0.06

Table 10: Near-Field Records, Roof Drift Demands of 3D 5-, 8-, 12-storey building models (%)

			3D					
			5-Storey		8-Storey		12-Storey	
			X	**Y**	**X**	**Y**	**X**	**Y**
70	ImperialValley06_Chihuaua_282	Near Field	0.65	0.64	0.53	0.51	0.47	0.48
71	ImperialValley06_Chihuaua_V	Near Field	0.13	0.13	0.07	0.08	0.04	0.04
72	ImperialValley06_ElCentroArray6_140	Near Field	0.82	0.81	0.51	0.60	0.62	0.63
73	ImperialValley06_ElCentroArray6_230	Near Field	2.38	2.36	0.67	0.70	2.44	2.47
74	ImperialValley06_ElCentroArray6_V	Near Field	0.73	0.73	0.38	0.41	0.56	0.57
75	ImperialValley06_ElCentroArray7_140	Near Field	0.72	0.72	0.82	0.87	0.40	0.40
76	ImperialValley06_ElCentroArray7_230	Near Field	2.59	2.58	1.07	1.09	1.89	1.92
77	ImperialValley06_ElCentroArray7_V	Near Field	0.21	0.21	0.23	0.41	0.29	0.30
78	ImperialValley06_BondaCorner_140	Near Field	0.08	0.08	0.04	0.04	0.02	0.02
79	ImperialValley06_BondaCorner_230	Near Field	0.17	0.17	0.13	0.13	0.09	0.09
80	ImperialValley06_BondaCorner_V	Near Field	0.00	0.00	0.00	0.00	0.00	0.00
81	IrpiniaItaly_Sturno_00	Near Field	0.50	0.50	0.30	0.30	0.31	0.30
82	IrpiniaItaly_Sturno_230	Near Field	1.13	1.12	0.43	0.46	0.83	0.85
83	IrpiniaItaly_Sturno_V	Near Field	0.20	0.20	0.14	0.16	0.27	0.28
84	NahanniCanada_Site1_10	Near Field	0.42	0.42	0.56	0.50	0.37	0.38

`

Table 11: Near-Field Records, Roof Drift Demands of 2D 5-, 8-, 12-storey building models (%)

			2D					
			5-Storey		8-Storey		12-Storey	
			X	Y	X	Y	X	Y
70	ImperialValley06_Chihuaua_282	Near Field	0.50	0.50	0.51	0.35	0.55	0.27
71	ImperialValley06_Chihuaua_V	Near Field	0.07	0.07	0.08	0.05	0.06	0.04
72	ImperialValley06_ElCentroArray6_140	Near Field	0.54	0.54	0.64	0.33	1.13	0.29
73	ImperialValley06_ElCentroArray6_230	Near Field	1.21	1.21	0.51	0.32	1.83	0.39
74	ImperialValley06_ElCentroArray6_V	Near Field	0.50	0.50	0.34	0.24	0.52	0.20
75	ImperialValley06_ElCentroArray7_140	Near Field	0.42	0.42	0.69	0.30	0.56	0.20
76	ImperialValley06_ElCentroArray7_230	Near Field	2.01	2.01	1.02	0.52	1.52	0.78
77	ImperialValley06_ElCentroArray7_V	Near Field	0.25	0.25	0.16	0.16	0.31	0.10
78	ImperialValley06_BondaCorner_140	Near Field	0.07	0.07	0.04	0.05	0.02	0.03
79	ImperialValley06_BondaCorner_230	Near Field	0.11	0.11	0.13	0.08	0.09	0.06
80	ImperialValley06_BondaCorner_V	Near Field	0.00	0.00	0.00	0.00	0.00	0.00
81	IrpiniaItaly_Sturno_00	Near Field	0.37	0.37	0.29	0.27	0.42	0.20
82	IrpiniaItaly_Sturno_230	Near Field	0.33	0.33	0.35	0.19	0.77	0.14
83	IrpiniaItaly_Sturno_V	Near Field	0.14	0.14	0.11	0.09	0.26	0.06
84	NahanniCanada_Site1_10	Near Field	0.30	0.30	0.40	0.38	0.47	0.16

The above tables are examples from the results of roof drift demands for 3D and 2D nonlinear building models. Whole table of calculated values can be found on APPENDIX. If we observe the values, we can see that near-field earthquake records show higher demand value estimates compared with far-field records on both 2D and 3D nonlinear building models. This is due to the fact that near-field records generally include strong, pulse-like ground motions that are not typically present in far-field records. They also contain higher energy at lower frequencies compared to far-field waves.

4.5 Results and discussions

In this study three low to mid-rise buildings, 5-, 8-, and 12-storey respectively were taken into consideration. Nonlinear static analyses were performed on 2D and 3D frames. Six static pushover curves were obtained from 3D building models, one on each principal direction. Also, six static pushover curves were obtained from 2D

`

building models. A total of twelve pushover curves were obtained from ETABS. 2D and 3D model pushover curves in X and Y direction were compared with each other in order to see how these building models reflect typical real-life premodern reinforced concrete building behavior.

The main focus of this study was to compare displacement demands of the three buildings. Displacement demands were obtained from performing time history analyses on 2D and 3D models. Each pushover curve was bi-linearized in order to continue with time history analysis process. A total of 147 earthquakes, including far-field and near-field records were used in order to perform time histories. A total of 1764 time histories were ran in NONLIN software. The output taken from the program was the displacement. After doing all the necessary calculations as explained in methodology part, the final roof drift ratio in percentage was calculated for each model on both directions.

Table 12: Maximum and average roof drift values for 3D models in both directions (%)

	ROOF DRIFT (%)					
	5S-3D-X	**5S-3D-Y**	**8S-3D-X**	**8S-3D-Y**	**12S-3D-X**	**12S-3D-Y**
MAXIMUM	4.565	4.541	3.087	2.914	2.438	2.472
AVERAGE	0.811	0.807	0.468	0.494	0.535	0.544

Table 13: Maximum and average roof drift values for 2D models in both directions (%)

	ROOF DRIFT (%)					
	5S-2D-X	**5S-2D-Y**	**8S-2D-X**	**8S-2D-Y**	**12S-2D-X**	**12S-2D-Y**
MAXIMUM	5.897	5.897	3.978	2.063	2.100	2.760
AVERAGE	0.627	0.627	0.445	0.309	0.562	0.264

For each earthquake record, the roof drift was calculated n each direction. To derive insights from the data, both the average and maximum roof drift values were

`

determined for each configuration, illustrated in both *Table 12* and *Table 13*. The average values provide a general idea of the typical building behavior under seismic loads. They offer a baseline for expected performance. On the other hand, the maximum values highlight the extreme performance scenarios. They capture the worst-case conditions that a building might experience during an earthquake event.

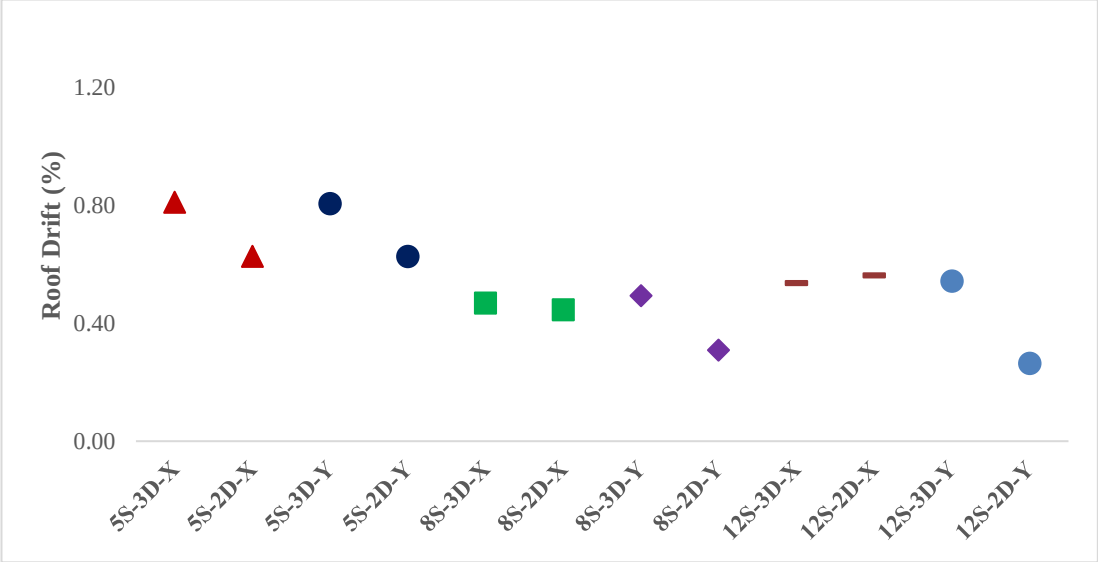

Figure 25: Average Roof Drift (%)

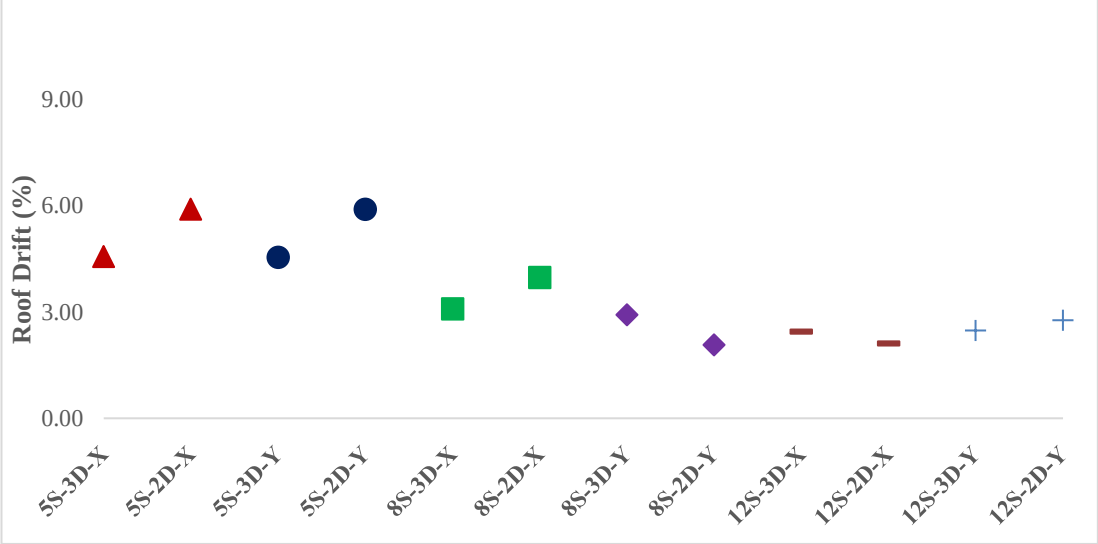

Figure 26: Maximum Roof Drift (%)

`

Comparing maximum and average drift ratios is important in determining how 2D models reflect their 3D counterparts. *Figure 25* show how these building models would typically behave under seismic events. Considering 5-storey building, the difference in percentage of the roof drift between 3D and 2D models is 0.18% in both x and y directions. Taking into consideration 8-storey building, the difference in roof drifts is 0.023% in x direction and 0.185% in y direction. As for the 12-storey building, this difference in x direction is 0.027% in x and 0.28% in y direction. The comparison of average roof drift demands for 2D and 3D models shown in *Figure 25*, indicates that 2D models reflect reasonably well their respective 3D models.

Figure 26 shows maximum roof drift demand of 2D and 3D nonlinear building models. Maximum values describe the worst-case scenario that can happen during earthquake events. Considering 5-storey building, the difference between maximum roof drift between 3D and 2D models is 1.332% in x direction and 1.356% in y direction. For 8-storey building, this difference is 0.891% and 0.851% in x and y directions respectively. Considering 12-storey building, the difference in x direction is 0.038% and 0.288% in y direction. So, it can be concluded that 2D models represent really well 3D models even in most adverse situations.

`

CHAPTER 5

CONCLUSIONS

5.1 Conclusions

This study focused on assessing the seismic behavior of reinforced concrete buildings using both 2D and 3D modeling techniques. Three buildings of varying heights (5, 8, and 12 stories) were analyzed to compare the displacement demands derived from pushover and time history analyses under seismic loads. The main findings from this study can be summarized as follows:

- Displacement demands obtained from time history analyses revealed that the maximum and average roof drift values were slightly higher for 3D models compared to 2D models across all building heights.
- The average roof drift values for both 2D and 3D models provided a general idea of typical building behavior under seismic loads, serving as a baseline for expected performance. Considering 5-storey building, the difference in average roof drift between 2D and 3D models in both directions is 0.18%. Considering 8-storey building, the difference of roof drift is 0.023% and 0.185% in x and y directions respectively. As for the 12-storey building, these differences are 0.027% in x direction and 0.28% in y direction. The maximum roof drift values, on the other hand, highlighted the extreme performance scenarios, capturing the worst-case conditions that buildings might experience during an earthquake.
- The comparison of roof drift demands showed that 2D models reflect the behavior of 3D models reasonably well. This demonstrates the reliability of using 2D models for seismic analysis, especially when computational resources or time constraints are critical factors. For instance, considering the 5-storey building, the difference in maximum roof drift between 3D and 2D models is 1.332% in x and 1.356% in y direction. For the 8-storey building, this difference is 0.891% and

`

0.851% in the x and y directions, respectively. For the 12-storey building, the difference in x direction is 0.038% and 0.288% in y direction.

- The findings of this study support the use of 2D models in practical engineering applications for the seismic analysis of reinforced concrete frames. While 3D models offer more detailed insights, 2D models provide a sufficient level of accuracy for preliminary assessments.

In conclusion, this thesis demonstrates that while 3D models remain the standard for detailed seismic analysis, 2D models are valuable tools that can simplify the assessment process without significantly compromising accuracy.

5.2 Recommendations for future research

Based on the findings of this study, future studies should include a wider variety of building types and heights to provide a more comprehensive understanding of the applicability of 2D models across different structural configurations. Also, a more complex soil-structure interaction effect and examining the influence of different material properties on seismic response should also be considered. Additionally, future research should investigate how shear and infill walls effect on how 2D models reflect their respective 3D models. These future research directions will contribute to a more accurate and reliable seismic assessment framework for reinforced concrete buildings.

`

REFERENCES

[1] M. Hysenlliu, H. Bilgin, A. Bidaj and M. Leti, "Structural performance of URM school buildings during the 2019 Albania earthquakes," *CHALLENGE JOURNAL OF STRUCTURAL MECHANICS,* vol. 6, no. 4, pp. 215-231, December 2020.

[2] E. Işık, F. Avcil, R. İzol, A. Büyüksaraç, H. Bilgin, E. Harirchian and E. Arkan, "Field Reconnaissance and Earthquake Vulnerability of the RC Buildings in Adıyaman during 2023 Türkiye Earthquakes," *Applied Sciences,* vol. 14, no. 7, p. 2860, 2024.

[3] CSI, ETABS, Integrated Building Design Software, Berkeley, 2002.

[4] F. A. Charney and B. Brangrover, "NONLIN: Software for Earthquake Engineering Education," in *Structures Congress 2004,* Blacksburg, 2004.

[5] A. S. Elnashai and L. Di Sarno, Fundamentals of EARTHQUAKE ENGINEERING, Chichester: Wiley, 2008.

[6] F. Naeim, The Seismic Design Handbook, 2nd ed., New York: Kluwer Academic Publishers, 2001.

[7] R. Alderliesten, "Types of Structuraal Loads," LibreTexts , 12 April 2021. [Online]. Available: https://shorturl.at/jyEa7.

[8] CSI, SAP2000 V-19, Integrated Solutions for Structural Analysis and Design, Berkeley, California, 2016.

[9] CEN, "Eurocode 8: Design of structures for earthquake resistance - Part 1: General rules, seismic actions and rules for buildings". Belgium December 2004.

[10] T. Lu and G. Hu, "Review on Baseline Correction of Strong-Motion Accelerogram," *East Asian Science Technology and Society International Journal,* vol. 3, no. 6, pp. 309-314, 2016.

[11] R. Bento, S. S. Falcão and F. B. Rodrigues, "Non-Linear Static Procedures in Performance Based Seismic Design," in *13th World Conference on Earthquake Engineering,* Vancouver, 2004.

`

[12] Prasad, "Pushover Analysis: Structural Advanced Simulations," Structural Guide, [Online]. Available: https://www.structuralguide.com/pushover-analysis/.

[13] A. S. E. Elnashai, "Advanced inelastic static (pushover) analysis for earthquake applications," *Structural Engineering and Mechanics,* vol. 12, no. 1, pp. 51-69, 2001.

[14] M. İnel and H. B. Özmen, "Effects of plastic hinge properties in nonlinear analysis of reinforced concrete bildings," *Engineering Structures,* vol. 28, no. 11, pp. 1494-1502, 2006.

[15] H. Krawinkler and G. Seneviratna, "Pros and cons of a pushover analysis of seismic performance evaluation," *Engineering Structures,* vol. 20, no. 4, pp. 452-464, 1998.

[16] D. Vamvatsikos and C. Cornell, "Incremental Dynamic Analysis," *Earthquake Engineering & Structural Dynamics,* vol. 31, no. 3, pp. 491-514, 2002.

[17] E. Özer, M. Kamal and M. İnel, "Comparison of Linear and Nonlinear Seismic Behavior of 2D and 3D RC Buildings," *International Journal Of Engineering & Applied Sciences,* vol. 9, no. 4, pp. 17-27, 2017.

[18] A. Hasan, K. I. M. Iqbal, S. Ahammed and A. Ghosh, "Nonlinear Time History Analysis for Seismic Effects on Reinforced Concrete Building," *Nigerian Journal of Technological Development,* vol. 19, no. 4, pp. 391-399, 2022.

[19] CSI, ETABS, Analysis and Design of Building Systems, CSi, 2021.

[20] M. Cosic, "About the Required Capacity of Nonlinear Deformations of the SDOF System with the Pushover Analysis," in *IConSSM* , Palic, 2009.

[21] A. Tsiavos and B. Stojadinovic, "Constant yield displacement procedure for seismic evaluation of existing structures," *Bulletin of Earthquake Engineering,* vol. 17, pp. 2137-2164, 2018.

[22] FEMA, Prestandard and Commentary For the Seismic Rehabilitation of Buildings, Reston, Virginia, 2000.

[23] Seismic Evaluation and Retrofit of Concrete Buildings, VOLUME I, Redwood: Applied Technology council, 1996.

`

[24] M. Inel, H. B. Ozmen and H. Bilgin, "Re-evaluation of building damage during recent earthquakes in Turkey," *Engineering Structures*, vol. 30, no. 2, pp. 412-427, 2008.

[25] M. Hysenlliu, H. Bilgin, A. Bidaj and M. Leti, "Structural performance of URM school buildings during the 2019 Albania earthquakes," *Challange Journal of Structural Mechanics*, vol. 6, no. 4, pp. 215-231, December 2020.

`

APPENDIX

Table 14: Parameters used to perform nonlinear time histroy analyses on NONLIN

5-Storey 3D-X											
	Earthquake	Type	dy	Vy	W	c	α	k1	k2	σ	δ
			[m]	[kN]	[kN]	[%]		[kN/m]	[kN/m]	[kN]	[m]
1	SanFernando_LA_HollywoodStor_90	Farfield	0.02	980	7843.5	5	0.83	65333.33	0.00	1180.72	0.03
2	SanFernando_LA_HollywoodStor_180	Farfield	0.02	980	7843.5	5	0.83	65333.33	0.00	1180.72	0.02
3	SanFernando_LA_HollywoodStor_V	Farfield	0.02	980	7843.5	5	0.83	65333.33	0.00	1180.72	0.01
4	Friuli-Italy-Tolmezzo_00	Farfield	0.02	980	7843.5	5	0.83	65333.33	0.00	1180.72	0.03
5	Friuli-Italy-Tolmezzo_270	Farfield	0.02	980	7843.5	5	0.83	65333.33	0.00	1180.72	0.07
6	Friuli-Italy-Tolmezzo_V	Farfield	0.02	980	7843.5	5	0.83	65333.33	0.00	1180.72	0.01
7	ImperialValley-06_Delta_262	Farfield	0.02	980	7843.5	5	0.83	65333.33	0.00	1180.72	0.09
8	ImperialValley-06_Delta_352	Farfield	0.02	980	7843.5	5	0.83	65333.33	0.00	1180.72	0.09
9	ImperialValley-06_Delta_V	Farfield	0.02	980	7843.5	5	0.83	65333.33	0.00	1180.72	0.01
10	ImperialValley-06_Delta_ElCentro11_140	Farfield	0.02	980	7843.5	5	0.83	65333.33	0.00	1180.72	0.07
11	ImperialValley-06_Delta_ElCentro11_230	Farfield	0.02	980	7843.5	5	0.83	65333.33	0.00	1180.72	0.04
12	ImperialValley-06_Delta_ElCentro11_V	Farfield	0.02	980	7843.5	5	0.83	65333.33	0.00	1180.72	0.01
13	SuperstitionHills02_ElCentromp_00	Farfield	0.02	980	7843.5	5	0.83	65333.33	0.00	1180.72	0.12
14	SuperstitionHills02_ElCentromp_90	Farfield	0.02	980	7843.5	5	0.83	65333.33	0.00	1180.72	0.04
15	SuperstitionHills02_ElCentromp_V	Farfield	0.02	980	7843.5	5	0.83	65333.33	0.00	1180.72	0.02
16	SuperstitionHills02_PeoRoad_270	Farfield	0.02	980	7843.5	5	0.83	65333.33	0.00	1180.72	0.08
17	SuperstitionHills02_PoeRoad_360	Farfield	0.02	980	7843.5	5	0.83	65333.33	0.00	1180.72	0.04
18	LomaPrieta_Capitola_00	Farfield	0.02	980	7843.5	5	0.83	65333.33	0.00	1180.72	0.09
19	LomaPrieta_Capitola_90	Farfield	0.02	980	7843.5	5	0.83	65333.33	0.00	1180.72	0.10
20	LomaPrieta_Capitola_V	Farfield	0.02	980	7843.5	5	0.83	65333.33	0.00	1180.72	0.03
21	LomaPrieta_GilroyArray3_00	Farfield	0.02	980	7843.5	5	0.83	65333.33	0.00	1180.72	0.06
22	LomaPrieta_GilroyArray3_90	Farfield	0.02	980	7843.5	5	0.83	65333.33	0.00	1180.72	0.08
23	LomaPrieta_GilroyArray3_V	Farfield	0.02	980	7843.5	5	0.83	65333.33	0.00	1180.72	0.01
24	CapeMendocino_RioDellOverpass_360	Farfield	0.02	980	7843.5	5	0.83	65333.33	0.00	1180.72	0.06
25	CapeMendocino_RioDellOverpass_Vertical	Farfield	0.02	980	7843.5	5	0.83	65333.33	0.00	1180.72	0.03
26	CapeMendocino_RioDellOverpass_270	Farfield	0.02	980	7843.5	5	0.83	65333.33	0.00	1180.72	0.03
27	Landers_Coolwater_LN	Farfield	0.02	980	7843.5	5	0.83	65333.33	0.00	1180.72	0.08
28	Landers_Coolwater_TR	Farfield	0.02	980	7843.5	5	0.83	65333.33	0.00	1180.72	0.15
29	Landers_Coolwater_V	Farfield	0.02	980	7843.5	5	0.83	65333.33	0.00	1180.72	0.03
30	Landers_YermoFireStation_270	Farfield	0.02	980	7843.5	5	0.83	65333.33	0.00	1180.72	0.12
31	Landers_YermoFireStation_360	Farfield	0.02	980	7843.5	5	0.83	65333.33	0.00	1180.72	0.04
32	Landers_YermoFireStation_V	Farfield	0.02	980	7843.5	5	0.83	65333.33	0.00	1180.72	0.01
33	Northridge1_Beverlyhills12520_35	Farfield	0.02	980	7843.5	5	0.83	65333.33	0.00	1180.72	0.04
34	Northridge1_Beverlyhills12520_125	Farfield	0.02	980	7843.5	5	0.83	65333.33	0.00	1180.72	0.09
35	Northridge1_Beverlyhills12520_V	Farfield	0.02	980	7843.5	5	0.83	65333.33	0.00	1180.72	0.02
36	Northridge1_Beverlyhills14145_09	Farfield	0.02	980	7843.5	5	0.83	65333.33	0.00	1180.72	0.12

`

37	Northridge1_Beverlyhills14145_279	Farfield	0.02	980	7843.5	5	0.83	65333.33	0.00	1180.72	0.25
38	Northridge1_Beverlyhills14145_V	Farfield	0.02	980	7843.5	5	0.83	65333.33	0.00	1180.72	0.06
39	Northridge1_CanyonCountryWlostCanny_00	Farfield	0.02	980	7843.5	5	0.83	65333.33	0.00	1180.72	0.12
40	Northridge1_CanyonCountryWlostCanny_270	Farfield	0.02	980	7843.5	5	0.83	65333.33	0.00	1180.72	0.09
41	Northridge1_CanyonCountryWlostCanny_V	Farfield	0.02	980	7843.5	5	0.83	65333.33	0.00	1180.72	0.03
42	KobeJapan_NishiAkashi_00	Farfield	0.02	980	7843.5	5	0.83	65333.33	0.00	1180.72	0.07
43	KobeJapan_NishiAkashi_90	Farfield	0.02	980	7843.5	5	0.83	65333.33	0.00	1180.72	0.14
44	KobeJapan_NishiAkashi_V	Farfield	0.02	980	7843.5	5	0.83	65333.33	0.00	1180.72	0.03
45	KobeJapan_ShinOsaka_00	Farfield	0.02	980	7843.5	5	0.83	65333.33	0.00	1180.72	0.07
46	KobeJapan_ShinOsaka_90	Farfield	0.02	980	7843.5	5	0.83	65333.33	0.00	1180.72	0.06
47	KobeJapan_ShinOsaka_V	Farfield	0.02	980	7843.5	5	0.83	65333.33	0.00	1180.72	0.01
48	KocaeliTurkey_Arcelik_00	Farfield	0.02	980	7843.5	5	0.83	65333.33	0.00	1180.72	0.02
49	KocaeliTurkey_Arcelik_90	Farfield	0.02	980	7843.5	5	0.83	65333.33	0.00	1180.72	0.02
50	KocaeliTurkey_Arcelik_V	Farfield	0.02	980	7843.5	5	0.83	65333.33	0.00	1180.72	0.01
51	KocaeliTurkey_Duzce_180	Farfield	0.02	980	7843.5	5	0.83	65333.33	0.00	1180.72	0.10
52	KocaeliTurkey_Duzce_270	Farfield	0.02	980	7843.5	5	0.83	65333.33	0.00	1180.72	0.10
53	KocaeliTurkey_Duzce_V	Farfield	0.02	980	7843.5	5	0.83	65333.33	0.00	1180.72	0.02
54	ChiChiTaiwan_CHY101_E	Farfield	0.02	980	7843.5	5	0.83	65333.33	0.00	1180.72	0.12
55	ChiChiTaiwan_CHY101_N	Farfield	0.02	980	7843.5	5	0.83	65333.33	0.00	1180.72	0.30
56	ChiChiTaiwan_CHY101_Vertical	Farfield	0.02	980	7843.5	5	0.83	65333.33	0.00	1180.72	0.02
57	ChiChiTaiwan_CHY045_E	Farfield	0.02	980	7843.5	5	0.83	65333.33	0.00	1180.72	0.09
58	ChiChiTaiwan_CHY045_N	Farfield	0.02	980	7843.5	5	0.83	65333.33	0.00	1180.72	0.07
59	ChiChiTaiwan_CHY045_Vertical	Farfield	0.02	980	7843.5	5	0.83	65333.33	0.00	1180.72	0.03
60	DuzceTurkey_Bolu_00	Farfield	0.02	980	7843.5	5	0.83	65333.33	0.00	1180.72	0.13
61	DuzceTurkey_Bolu_90	Farfield	0.02	980	7843.5	5	0.83	65333.33	0.00	1180.72	0.15
62	DuzceTurkey_Bolu_Vertical	Farfield	0.02	980	7843.5	5	0.83	65333.33	0.00	1180.72	0.02
63	Manjillran_Abbar_L	Farfield	0.02	980	7843.5	5	0.83	65333.33	0.00	1180.72	0.08
64	Manjillran_Abbar_T	Farfield	0.02	980	7843.5	5	0.83	65333.33	0.00	1180.72	0.07
65	Manjillran_Abbar_V	Farfield	0.02	980	7843.5	5	0.83	65333.33	0.00	1180.72	0.07
66	HectorMine_Hector_00	Farfield	0.02	980	7843.5	5	0.83	65333.33	0.00	1180.72	0.04
67	HectorMine_Hector_90	Farfield	0.02	980	7843.5	5	0.83	65333.33	0.00	1180.72	0.07
68	HectorMine_Hector_V	Farfield	0.02	980	7843.5	5	0.83	65333.33	0.00	1180.72	0.02
69	ImperialValley06_Chihuaua_12	Nearfield	0.02	980	7843.5	5	0.83	65333.33	0.00	1180.72	0.05
70	ImperialValley06_Chihuaua_282	Nearfield	0.02	980	7843.5	5	0.83	65333.33	0.00	1180.72	0.08
71	ImperialValley06_Chihuaua_V	Nearfield	0.02	980	7843.5	5	0.83	65333.33	0.00	1180.72	0.02
72	ImperialValley06_ElCentroArray6_140	Nearfield	0.02	980	7843.5	5	0.83	65333.33	0.00	1180.72	0.10
73	ImperialValley06_ElCentroArray6_230	Nearfield	0.02	980	7843.5	5	0.83	65333.33	0.00	1180.72	0.28
74	ImperialValley06_ElCentroArray6_V	Nearfield	0.02	980	7843.5	5	0.83	65333.33	0.00	1180.72	0.09
75	ImperialValley06_ElCentroArray7_140	Nearfield	0.02	980	7843.5	5	0.83	65333.33	0.00	1180.72	0.08
76	ImperialValley06_ElCentroArray7_230	Nearfield	0.02	980	7843.5	5	0.83	65333.33	0.00	1180.72	0.30
77	ImperialValley06_ElCentroArray7_V	Nearfield	0.02	980	7843.5	5	0.83	65333.33	0.00	1180.72	0.02
78	ImperialValley06_BondaCorner_140	Nearfield	0.02	980	7843.5	5	0.83	65333.33	0.00	1180.72	0.01
79	ImperialValley06_BondaCorner_230	Nearfield	0.02	980	7843.5	5	0.83	65333.33	0.00	1180.72	0.02
80	ImperialValley06_BondaCorner_V	Nearfield	0.02	980	7843.5	5	0.83	65333.33	0.00	1180.72	0.00
81	IrpiniaItaly_Sturno_00	Nearfield	0.02	980	7843.5	5	0.83	65333.33	0.00	1180.72	0.06

`

82	IrpiniaItaly_Sturno_230	Nearfield	0.02	980	7843.5	5	0.83	65333.33	0.00	1180.72	0.13
83	IrpiniaItaly_Sturno_V	Nearfield	0.02	980	7843.5	5	0.83	65333.33	0.00	1180.72	0.02
84	NahanniCanada_Site1_10	Nearfield	0.02	980	7843.5	5	0.83	65333.33	0.00	1180.72	0.05
85	NahanniCanada_Site1_280	Nearfield	0.02	980	7843.5	5	0.83	65333.33	0.00	1180.72	0.05
86	NahanniCanada_Site1_V	Nearfield	0.02	980	7843.5	5	0.83	65333.33	0.00	1180.72	0.09
87	NahanniCanada_Site2_240	Nearfield	0.02	980	7843.5	5	0.83	65333.33	0.00	1180.72	0.03
88	NahanniCanada_Site2_330	Nearfield	0.02	980	7843.5	5	0.83	65333.33	0.00	1180.72	0.05
89	SuperstitionHills02_ParachuteTestSite_225	Nearfield	0.02	980	7843.5	5	0.83	65333.33	0.00	1180.72	0.32
90	SuperstitionHills02_ParachuteTestSite_315	Nearfield	0.02	980	7843.5	5	0.83	65333.33	0.00	1180.72	0.10
91	LomaPrieta_Bran_00	Nearfield	0.02	980	7843.5	5	0.83	65333.33	0.00	1180.72	0.12
92	LomaPrieta_Bran_90	Nearfield	0.02	980	7843.5	5	0.83	65333.33	0.00	1180.72	0.20
93	LomaPrieta_Bran_V	Nearfield	0.02	980	7843.5	5	0.83	65333.33	0.00	1180.72	0.02
94	LomaPrieta_Corralitos_00	Nearfield	0.02	980	7843.5	5	0.83	65333.33	0.00	1180.72	0.19
95	LomaPrieta_Corralitos_90	Nearfield	0.02	980	7843.5	5	0.83	65333.33	0.00	1180.72	0.10
96	LomaPrieta_Corralitos_V	Nearfield	0.02	980	7843.5	5	0.83	65333.33	0.00	1180.72	0.04
97	LomaPrieta_SaratogaAloha_00	Nearfield	0.02	980	7843.5	5	0.83	65333.33	0.00	1180.72	0.14
98	LomaPrieta_SaratogaAloha_90	Nearfield	0.02	980	7843.5	5	0.83	65333.33	0.00	1180.72	0.04
99	LomaPrieta_SaratogaAloha_V	Nearfield	0.02	980	7843.5	5	0.83	65333.33	0.00	1180.72	0.04
100	ErzicanTurkey_Erzincan_EW	Nearfield	0.02	980	7843.5	5	0.83	65333.33	0.00	1180.72	0.19
101	ErzicanTurkey_Erzincan_NS	Nearfield	0.02	980	7843.5	5	0.83	65333.33	0.00	1180.72	0.35
102	ErzicanTurkey_Erzincan_V	Nearfield	0.02	980	7843.5	5	0.83	65333.33	0.00	1180.72	0.02
103	CapeMendocino_CapeMendocino_00	Nearfield	0.02	980	7843.5	5	0.83	65333.33	0.00	1180.72	0.22
104	CapeMendocino_CapeMendocino_90	Nearfield	0.02	980	7843.5	5	0.83	65333.33	0.00	1180.72	0.07
105	CapeMendocino_CapeMendocino_V	Nearfield	0.02	980	7843.5	5	0.83	65333.33	0.00	1180.72	0.14
106	CapeMendocino_Petrolia_00	Nearfield	0.02	980	7843.5	5	0.83	65333.33	0.00	1180.72	0.14
107	CapeMendocino_Petrolia_90	Nearfield	0.02	980	7843.5	5	0.83	65333.33	0.00	1180.72	0.26
108	CapeMendocino_Petrolia_V	Nearfield	0.02	980	7843.5	5	0.83	65333.33	0.00	1180.72	0.02
109	Landers_Lucerne_260	Nearfield	0.02	980	7843.5	5	0.83	65333.33	0.00	1180.72	0.26
110	Landers_Lucerne_345	Nearfield	0.02	980	7843.5	5	0.83	65333.33	0.00	1180.72	0.04
111	Landers_Lucerne_V	Nearfield	0.02	980	7843.5	5	0.83	65333.33	0.00	1180.72	0.08
112	Northridge01_Lasepulveda_270	Nearfield	0.02	980	7843.5	5	0.83	65333.33	0.00	1180.72	0.18
113	Northridge01_Lasepulveda_360	Nearfield	0.02	980	7843.5	5	0.83	65333.33	0.00	1180.72	0.09
114	Northridge01_Lasepulveda_V	Nearfield	0.02	980	7843.5	5	0.83	65333.33	0.00	1180.72	0.07
115	Northridge01_1765SaticoySt_90	Nearfield	0.02	980	7843.5	5	0.83	65333.33	0.00	1180.72	0.06
116	Northridge01_1765SaticoySt_180	Nearfield	0.02	980	7843.5	5	0.83	65333.33	0.00	1180.72	0.19
117	Northridge01_RinaldiReceivingSta_228	Nearfield	0.02	980	7843.5	5	0.83	65333.33	0.00	1180.72	0.24
118	Northridge01_RinaldiReceivingSta_318	Nearfield	0.02	980	7843.5	5	0.83	65333.33	0.00	1180.72	0.14
119	Northridge01_RinaldiReceivingSta_V	Nearfield	0.02	980	7843.5	5	0.83	65333.33	0.00	1180.72	0.04
120	Northridge01_SylmarOliveView_90	Nearfield	0.02	980	7843.5	5	0.83	65333.33	0.00	1180.72	0.19
121	Northridge01_SylmarOliveView_360	Nearfield	0.02	980	7843.5	5	0.83	65333.33	0.00	1180.72	0.28
122	Northridge01_SylmarOliveView_V	Nearfield	0.02	980	7843.5	5	0.83	65333.33	0.00	1180.72	0.06
123	KocaeliTurkey_Izmit_90	Nearfield	0.02	980	7843.5	5	0.83	65333.33	0.00	1180.72	0.05
124	KocaeliTurkey_Izmit_180	Nearfield	0.02	980	7843.5	5	0.83	65333.33	0.00	1180.72	0.04
125	KocaeliTurkey_Izmit_V	Nearfield	0.02	980	7843.5	5	0.83	65333.33	0.00	1180.72	0.02
126	KocaeliTurkey_Yamica_30	Nearfield	0.02	980	7843.5	5	0.83	65333.33	0.00	1180.72	0.12

`

127	KocaeliTurkey_Yamica_60	Nearfield	0.02	980	7843.5	5	0.83	65333.33	0.00	1180.72	0.09
128	KocaeliTurkey_Yamica_V	Nearfield	0.02	980	7843.5	5	0.83	65333.33	0.00	1180.72	0.04
129	ChiChiTaiwan_TCU065_E	Nearfield	0.02	980	7843.5	5	0.83	65333.33	0.00	1180.72	0.28
130	ChiChiTaiwan_TCU065_N	Nearfield	0.02	980	7843.5	5	0.83	65333.33	0.00	1180.72	0.37
131	ChiChiTaiwan_TCU065_V	Nearfield	0.02	980	7843.5	5	0.83	65333.33	0.00	1180.72	0.06
132	ChiChiTaiwan_TCU067_E	Nearfield	0.02	980	7843.5	5	0.83	65333.33	0.00	1180.72	0.14
133	ChiChiTaiwan_TCU067_N	Nearfield	0.02	980	7843.5	5	0.83	65333.33	0.00	1180.72	0.11
134	ChiChiTaiwan_TCU067_V	Nearfield	0.02	980	7843.5	5	0.83	65333.33	0.00	1180.72	0.06
135	ChiChiTaiwan_TCU084_E	Nearfield	0.02	980	7843.5	5	0.83	65333.33	0.00	1180.72	0.53
136	ChiChiTaiwan_TCU084_N	Nearfield	0.02	980	7843.5	5	0.83	65333.33	0.00	1180.72	0.19
137	ChiChiTaiwan_TCU084_V	Nearfield	0.02	980	7843.5	5	0.83	65333.33	0.00	1180.72	0.07
138	ChiChiTaiwan_TCU102_E	Nearfield	0.02	980	7843.5	5	0.83	65333.33	0.00	1180.72	0.30
139	ChiChiTaiwan_TCU102_N	Nearfield	0.02	980	7843.5	5	0.83	65333.33	0.00	1180.72	0.08
140	ChiChiTaiwan_TCU102_V	Nearfield	0.02	980	7843.5	5	0.83	65333.33	0.00	1180.72	0.03
141	DuzceTurkey_Duzce_180	Nearfield	0.02	980	7843.5	5	0.83	65333.33	0.00	1180.72	0.09
142	DuzceTurkey_Duzce_270	Nearfield	0.02	980	7843.5	5	0.83	65333.33	0.00	1180.72	0.15
143	DuzceTurkey_Duzce_V	Nearfield	0.02	980	7843.5	5	0.83	65333.33	0.00	1180.72	0.02
144	DenaliAlaska_TAPSPumpStation10_47	Nearfield	0.02	980	7843.5	5	0.83	65333.33	0.00	1180.72	0.20
145	DenaliAlaska_TAPSPumpStation10_317	Nearfield	0.02	980	7843.5	5	0.83	65333.33	0.00	1180.72	0.13
146	DenaliAlaska_TAPSPumpStation10_V	Nearfield	0.02	980	7843.5	5	0.83	65333.33	0.00	1180.72	0.05

`

Table 15: Roof Drift Demand (%) for 3D building models

			Roof Drift Demand 3D					
			5-Storey		8-Storey		12-Storey	
	Earthquake	**Type**	**X**	**Y**	**X**	**Y**	**X**	**Y**
1	SanFernando_LA_HollywoodStor_90	Far Field	0.23	0.23	0.33	0.31	0.20	0.21
2	SanFernando_LA_HollywoodStor_180	Far Field	0.18	0.18	0.14	0.16	0.11	0.12
3	SanFernando_LA_HollywoodStor_V	Far Field	0.06	0.06	0.07	0.06	0.06	0.06
4	Friuli-Italy-Tolmezzo_00	Far Field	0.29	0.29	0.29	0.27	0.25	0.26
5	Friuli-Italy-Tolmezzo_270	Far Field	0.64	0.63	0.40	0.39	0.20	0.20
6	Friuli-Italy-Tolmezzo_V	Far Field	0.09	0.09	0.07	0.09	0.06	0.06
7	ImperialValley-06_Delta_262	Far Field	0.76	0.75	0.40	0.41	0.27	0.27
8	ImperialValley-06_Delta_352	Far Field	0.75	0.75	0.45	0.47	0.41	0.43
9	ImperialValley-06_Delta_V	Far Field	0.11	0.11	0.07	0.07	0.10	0.10
10	ImperialValley-06_Delta_ElCentro11_140	Far Field	0.57	0.57	0.28	0.27	0.44	0.45
11	ImperialValley-06_Delta_ElCentro11_230	Far Field	0.37	0.37	0.26	0.26	0.50	0.50
12	ImperialValley-06_Delta_ElCentro11_V	Far Field	0.06	0.06	0.06	0.07	0.05	0.05
13	SuperstitionHills02_ElCentromp_00	Far Field	1.00	0.99	0.51	0.53	0.41	0.42
14	SuperstitionHills02_ElCentromp_90	Far Field	0.34	0.34	0.16	0.17	0.36	0.36
15	SuperstitionHills02_ElCentromp_V	Far Field	0.13	0.13	0.13	0.13	0.08	0.08
16	SuperstitionHills02_PeoRoad_270	Far Field	0.71	0.70	0.37	0.38	0.26	0.26
17	SuperstitionHills02_PoeRoad_360	Far Field	0.36	0.36	0.35	0.33	0.28	0.29
18	LomaPrieta_Capitola_00	Far Field	0.80	0.80	0.51	0.53	0.71	0.74
19	LomaPrieta_Capitola_90	Far Field	0.88	0.87	0.39	0.38	0.39	0.39
20	LomaPrieta_Capitola_V	Far Field	0.22	0.21	0.14	0.16	0.12	0.12
21	LomaPrieta_GilroyArray3_00	Far Field	0.54	0.54	0.40	0.40	0.21	0.21
22	LomaPrieta_GilroyArray3_90	Far Field	0.65	0.65	0.40	0.43	0.71	0.72
23	LomaPrieta_GilroyArray3_V	Far Field	0.07	0.07	0.08	0.10	0.16	0.16
24	CapeMendocino_RioDellOverpass_360	Far Field	0.53	0.52	0.34	0.34	0.50	0.51
25	CapeMendocino_RioDellOverpass_Vertical	Far Field	0.24	0.24	0.19	0.22	0.20	0.21
26	CapeMendocino_RioDellOverpass_270	Far Field	0.24	0.24	0.19	0.22	0.20	0.21
27	Landers_Coolwater_LN	Far Field	0.70	0.69	0.38	0.34	0.28	0.28
28	Landers_Coolwater_TR	Far Field	1.27	1.27	0.43	0.41	0.81	0.81
29	Landers_Coolwater_V	Far Field	0.22	0.22	0.09	0.09	0.09	0.09
30	Landers_YermoFireStation_270	Far Field	1.03	1.03	0.38	0.38	0.92	0.94
31	Landers_YermoFireStation_360	Far Field	0.30	0.30	0.28	0.32	0.33	0.33
32	Landers_YermoFireStation_V	Far Field	0.09	0.09	0.12	0.14	0.14	0.14
33	Northridge1_Beverlyhills12520_35	Far Field	0.37	0.37	0.49	0.44	0.35	0.36
34	Northridge1_Beverlyhills12520_125	Far Field	0.74	0.74	0.31	0.31	0.21	0.22
35	Northridge1_Beverlyhills12520_V	Far Field	0.16	0.16	0.13	0.13	0.16	0.16
36	Northridge1_Beverlyhills14145_09	Far Field	1.02	1.01	0.63	0.77	1.08	1.10
37	Northridge1_Beverlyhills14145_279	Far Field	2.11	2.10	1.06	1.12	0.78	0.79
38	Northridge1_Beverlyhills14145_V	Far Field	0.53	0.52	0.47	0.47	0.15	0.15
39	Northridge1_CanyonCountryWlostCanny_00	Far Field	1.06	1.05	0.48	0.53	0.67	0.69
40	Northridge1_CanyonCountryWlostCanny_270	Far Field	0.73	0.73	0.52	0.54	0.45	0.46
41	Northridge1_CanyonCountryWlostCanny_V	Far Field	0.22	0.22	0.12	0.13	0.14	0.14
42	KobeJapan_NishiAkashi_00	Far Field	0.59	0.59	0.44	0.44	0.28	0.27
43	KobeJapan_NishiAkashi_90	Far Field	1.20	1.19	0.45	0.44	0.31	0.31
44	KobeJapan_NishiAkashi_V	Far Field	0.22	0.22	0.17	0.18	0.15	0.15

`

45	KobeJapan_ShinOsaka_00	Far Field	0.64	0.63	0.67	0.70	0.40	0.41
46	KobeJapan_ShinOsaka_90	Far Field	0.48	0.48	0.38	0.34	0.25	0.26
47	KobeJapan_ShinOsaka_V	Far Field	0.09	0.09	0.10	0.11	0.10	0.11
48	KocaeliTurkey_Arcelik_00	Far Field	0.17	0.17	0.18	0.16	0.12	0.13
49	KocaeliTurkey_Arcelik_90	Far Field	0.20	0.20	0.18	0.18	0.12	0.12
50	KocaeliTurkey_Arcelik_V	Far Field	0.08	0.08	0.05	0.06	0.07	0.13
51	KocaeliTurkey_Duzce_180	Far Field	0.83	0.82	0.46	0.50	0.64	0.65
52	KocaeliTurkey_Duzce_270	Far Field	0.83	0.82	0.45	0.49	0.62	0.62
53	KocaeliTurkey_Duzce_V	Far Field	0.13	0.13	0.15	0.17	0.13	0.13
54	ChiChiTaiwan_CHY101_E	Far Field	1.03	1.03	0.67	0.72	0.63	0.63
55	ChiChiTaiwan_CHY101_N	Far Field	2.62	2.60	1.38	1.46	1.35	1.38
56	ChiChiTaiwan_CHY101_Vertical	Far Field	0.16	0.16	0.14	0.16	0.23	0.24
57	ChiChiTaiwan_CHY045_E	Far Field	0.77	0.76	0.36	0.37	0.30	0.30
58	ChiChiTaiwan_CHY045_N	Far Field	0.59	0.58	0.55	0.60	0.32	0.32
59	ChiChiTaiwan_CHY045_Vertical	Far Field	0.24	0.24	0.28	0.30	0.20	0.21
60	DuzceTurkey_Bolu_00	Far Field	1.08	1.07	0.60	0.65	0.61	0.62
61	DuzceTurkey_Bolu_90	Far Field	1.30	1.29	1.24	1.14	0.54	0.54
62	DuzceTurkey_Bolu_Vertical	Far Field	0.18	0.18	0.18	0.20	0.17	0.17
63	Manjillran_Abbar_L	Far Field	0.66	0.66	0.44	0.46	0.33	0.34
64	Manjillran_Abbar_T	Far Field	0.59	0.58	0.41	0.47	0.51	0.52
65	Manjillran_Abbar_V	Far Field	0.62	0.62	0.31	0.31	0.53	0.54
66	HectorMine_Hector_00	Far Field	0.34	0.33	0.29	0.30	0.33	0.34
67	HectorMine_Hector_90	Far Field	0.61	0.61	0.33	0.37	0.60	0.60
68	HectorMine_Hector_V	Far Field	0.19	0.19	0.15	0.15	0.12	0.12
69	ImperialValley06_Chihuaua_12	Near Field	0.47	0.46	0.36	0.34	0.29	0.28
70	ImperialValley06_Chihuaua_282	Near Field	0.65	0.64	0.53	0.51	0.47	0.48
71	ImperialValley06_Chihuaua_V	Near Field	0.13	0.13	0.07	0.08	0.04	0.04
72	ImperialValley06_ElCentroArray6_140	Near Field	0.82	0.81	0.51	0.60	0.62	0.63
73	ImperialValley06_ElCentroArray6_230	Near Field	2.38	2.36	0.67	0.70	2.44	2.47
74	ImperialValley06_ElCentroArray6_V	Near Field	0.73	0.73	0.38	0.41	0.56	0.57
75	ImperialValley06_ElCentroArray7_140	Near Field	0.72	0.72	0.82	0.87	0.40	0.40
76	ImperialValley06_ElCentroArray7_230	Near Field	2.59	2.58	1.07	1.09	1.89	1.92
77	ImperialValley06_ElCentroArray7_V	Near Field	0.21	0.21	0.23	0.41	0.29	0.30
78	ImperialValley06_BondaCorner_140	Near Field	0.08	0.08	0.04	0.04	0.02	0.02
79	ImperialValley06_BondaCorner_230	Near Field	0.17	0.17	0.13	0.13	0.09	0.09
80	ImperialValley06_BondaCorner_V	Near Field	0.00	0.00	0.00	0.00	0.00	0.00
81	IrpiniaItaly_Sturno_00	Near Field	0.50	0.50	0.30	0.30	0.31	0.30
82	IrpiniaItaly_Sturno_230	Near Field	1.13	1.12	0.43	0.46	0.83	0.85
83	IrpiniaItaly_Sturno_V	Near Field	0.20	0.20	0.14	0.16	0.27	0.28
84	NahanniCanada_Site1_10	Near Field	0.42	0.42	0.56	0.50	0.37	0.38
85	NahanniCanada_Site1_280	Near Field	0.46	0.45	0.53	0.57	0.47	0.48
86	NahanniCanada_Site1_V	Near Field	0.75	0.75	0.49	0.59	0.34	0.35
87	NahanniCanada_Site2_240	Near Field	0.28	0.28	0.18	0.17	0.15	0.15
88	NahanniCanada_Site2_330	Near Field	0.43	0.43	0.39	0.39	0.23	0.23
89	SuperstitionHills02_ParachuteTestSite_225	Near Field	2.72	2.71	1.08	1.65	1.52	1.53
90	SuperstitionHills02_ParachuteTestSite_315	Near Field	0.85	0.85	0.45	0.40	0.61	0.62
91	LomaPrieta_Bran_00	Near Field	1.06	1.05	0.93	0.90	0.61	0.61
92	LomaPrieta_Bran_90	Near Field	1.71	1.70	0.80	0.71	0.34	0.35
93	LomaPrieta_Bran_V	Near Field	0.21	0.21	0.22	0.22	0.17	0.17
94	LomaPrieta_Corralitos_00	Near Field	1.65	1.64	0.49	0.51	0.42	0.43
95	LomaPrieta_Corralitos_90	Near Field	0.83	0.82	0.53	0.50	0.52	0.53

`

96	LomaPrieta_Corralitos_V	Near Field	0.34	0.34	0.19	0.18	0.17	0.18
97	LomaPrieta_SaratogaAloha_00	Near Field	1.19	1.18	0.44	0.47	0.31	0.31
98	LomaPrieta_SaratogaAloha_90	Near Field	0.31	0.31	0.30	0.36	0.24	0.24
99	LomaPrieta_SaratogaAloha_V	Near Field	0.32	0.32	0.23	0.27	0.25	0.26
100	ErzicanTurkey_Erzincan_EW	Near Field	1.63	1.62	0.80	0.87	0.56	0.57
101	ErzicanTurkey_Erzincan_NS	Near Field	3.02	3.01	1.24	1.40	1.75	1.77
102	ErzicanTurkey_Erzincan_V	Near Field	0.16	0.16	0.16	0.17	0.17	0.18
103	CapeMendocino_CapeMendocino_00	Near Field	1.89	1.88	0.82	0.91	1.19	1.20
104	CapeMendocino_CapeMendocino_90	Near Field	0.63	0.63	0.38	0.39	0.54	0.55
105	CapeMendocino_CapeMendocino_V	Near Field	1.21	1.20	0.39	0.42	0.94	0.97
106	CapeMendocino_Petrolia_00	Near Field	1.20	1.19	0.63	0.65	0.55	0.55
107	CapeMendocino_Petrolia_90	Near Field	2.24	2.23	0.91	1.00	1.39	1.41
108	CapeMendocino_Petrolia_V	Near Field	0.21	0.21	0.15	0.16	0.15	0.15
109	Landers_Lucerne_260	Near Field	2.23	2.22	0.56	0.51	2.18	2.22
110	Landers_Lucerne_345	Near Field	0.37	0.37	0.29	0.30	0.19	0.20
111	Landers_Lucerne_V	Near Field	0.66	0.66	0.29	0.33	0.57	0.58
112	Northridge01_Lasepulveda_270	Near Field	1.52	1.52	1.53	1.52	0.69	0.69
113	Northridge01_Lasepulveda_360	Near Field	0.79	0.79	0.64	0.85	0.62	0.63
114	Northridge01_Lasepulveda_V	Near Field	0.62	0.62	0.31	0.32	0.34	0.35
115	Northridge01_1765SaticoySt_90	Near Field	0.47	0.47	0.36	0.35	0.47	0.47
116	Northridge01_1765SaticoySt_180	Near Field	1.65	1.64	0.91	0.86	0.91	0.92
117	Northridge01_RinaldiReceivingSta_228	Near Field	2.04	2.03	1.93	1.87	1.42	1.44
118	Northridge01_RinaldiReceivingSta_318	Near Field	1.23	1.23	0.83	0.85	0.82	0.83
119	Northridge01_RinaldiReceivingSta_V	Near Field	0.36	0.36	0.37	0.39	0.31	0.31
120	Northridge01_SylmarOliveView_90	Near Field	1.60	1.59	1.06	1.09	1.14	1.14
121	Northridge01_SylmarOliveView_360	Near Field	2.37	2.36	1.04	1.10	1.15	1.17
122	Northridge01_SylmarOliveView_V	Near Field	0.49	0.49	0.28	0.30	0.22	0.22
123	KocaeliTurkey_Izmit_90	Near Field	0.45	0.45	0.25	0.27	0.31	0.32
124	KocaeliTurkey_Izmit_180	Near Field	0.31	0.31	0.23	0.27	0.29	0.30
125	KocaeliTurkey_Izmit_V	Near Field	0.14	0.14	0.07	0.08	0.13	0.13
126	KocaeliTurkey_Yamica_30	Near Field	1.05	1.05	0.51	0.55	0.80	0.82
127	KocaeliTurkey_Yamica_60	Near Field	0.78	0.77	0.49	0.45	0.74	0.74
128	KocaeliTurkey_Yamica_V	Near Field	0.36	0.36	0.31	0.33	0.35	0.35
129	ChiChiTaiwan_TCU065_E	Near Field	2.39	2.38	1.34	1.66	1.84	1.88
130	ChiChiTaiwan_TCU065_N	Near Field	3.17	3.15	1.34	1.66	1.94	1.95
131	ChiChiTaiwan_TCU065_V	Near Field	0.53	0.52	0.31	0.31	1.35	1.37
132	ChiChiTaiwan_TCU067_E	Near Field	1.24	1.23	0.81	0.82	2.03	2.09
133	ChiChiTaiwan_TCU067_N	Near Field	0.96	0.95	0.51	0.61	0.67	0.68
134	ChiChiTaiwan_TCU067_V	Near Field	0.53	0.52	0.30	0.31	0.28	0.28
135	ChiChiTaiwan_TCU084_E	Near Field	4.56	4.54	3.09	2.91	1.08	1.08
136	ChiChiTaiwan_TCU084_N	Near Field	1.62	1.61	0.90	1.00	0.74	0.74
137	ChiChiTaiwan_TCU084_V	Near Field	0.64	0.63	0.41	0.40	0.20	0.19
138	ChiChiTaiwan_TCU102_E	Near Field	2.58	2.57	0.57	0.63	1.77	1.79
139	ChiChiTaiwan_TCU102_N	Near Field	0.65	0.65	0.38	0.55	0.67	0.68
140	ChiChiTaiwan_TCU102_V	Near Field	0.28	0.27	0.25	0.30	0.90	0.92
141	DuzceTurkey_Duzce_180	Near Field	0.78	0.77	0.47	0.45	0.70	0.70
142	DuzceTurkey_Duzce_270	Near Field	1.28	1.28	0.65	0.79	0.81	0.81
143	DuzceTurkey_Duzce_V	Near Field	0.19	0.19	0.14	0.14	0.12	0.12
144	DenaliAlaska_TAPSPumpStation10_47	Near Field	1.71	1.70	1.02	1.03	1.71	1.74
145	DenaliAlaska_TAPSPumpStation10_317	Near Field	1.10	1.10	0.53	0.58	0.97	0.99
146	DenaliAlaska_TAPSPumpStation10_V	Near Field	0.39	0.39	0.23	0.24	0.54	0.54

`

Table 16: Roof Drift Demand (%) for 2D building models

			Roof Drift Demand 2D					
			5-Storey		8-Storey		12-Storey	
	Earthquake	**Type**	**X**	**Y**	**X**	**Y**	**X**	**Y**
1	SanFernando_LA_HollywoodStor_90	Far Field	0.25	0.25	0.19	0.15	0.35	0.10
2	SanFernando_LA_HollywoodStor_180	Far Field	0.16	0.16	0.11	0.10	0.13	0.06
3	SanFernando_LA_HollywoodStor_V	Far Field	0.05	0.05	0.05	0.03	0.12	0.02
4	Friuli-Italy-Tolmezzo_00	Far Field	0.30	0.30	0.28	0.19	0.28	0.11
5	Friuli-Italy-Tolmezzo_270	Far Field	0.54	0.54	0.46	0.49	0.22	0.23
6	Friuli-Italy-Tolmezzo_V	Far Field	0.08	0.08	0.06	0.05	0.07	0.04
7	ImperialValley-06_Delta_262	Far Field	0.27	0.27	0.43	0.24	0.26	0.17
8	ImperialValley-06_Delta_352	Far Field	0.40	0.40	0.36	0.40	0.43	0.17
9	ImperialValley-06_Delta_V	Far Field	0.08	0.08	0.09	0.05	0.11	0.04
10	ImperialValley-06_Delta_ElCentro11_140	Far Field	0.34	0.34	0.29	0.21	0.37	0.17
11	ImperialValley-06_Delta_ElCentro11_230	Far Field	0.27	0.27	0.39	0.28	0.34	0.19
12	ImperialValley-06_Delta_ElCentro11_V	Far Field	0.05	0.05	0.04	0.03	0.04	0.02
13	SuperstitionHills02_ElCentromp_00	Far Field	0.69	0.69	0.46	0.34	0.45	0.19
14	SuperstitionHills02_ElCentromp_90	Far Field	0.33	0.33	0.16	0.16	0.53	0.10
15	SuperstitionHills02_ElCentromp_V	Far Field	0.08	0.08	0.08	0.08	0.13	0.06
16	SuperstitionHills02_PeoRoad_270	Far Field	0.33	0.33	0.31	0.28	0.38	0.28
17	SuperstitionHills02_PoeRoad_360	Far Field	0.38	0.38	0.27	0.25	0.36	0.23
18	LomaPrieta_Capitola_00	Far Field	0.78	0.78	0.53	0.43	0.81	0.38
19	LomaPrieta_Capitola_90	Far Field	0.60	0.60	0.47	0.46	0.41	0.27
20	LomaPrieta_Capitola_V	Far Field	0.17	0.17	0.12	0.17	0.14	0.11
21	LomaPrieta_GilroyArray3_00	Far Field	0.37	0.37	0.40	0.33	0.22	0.17
22	LomaPrieta_GilroyArray3_90	Far Field	0.31	0.31	0.35	0.24	0.74	0.14
23	LomaPrieta_GilroyArray3_V	Far Field	0.12	0.12	0.05	0.07	0.29	0.04
24	CapeMendocino_RioDellOverpass_360	Far Field	0.59	0.59	0.34	0.40	0.50	0.26
25	CapeMendocino_RioDellOverpass_Vertical	Far Field	0.14	0.14	0.17	0.12	0.19	0.08
26	CapeMendocino_RioDellOverpass_270	Far Field	0.14	0.14	0.17	0.12	0.19	0.08
27	Landers_Coolwater_LN	Far Field	0.42	0.42	0.31	0.22	0.25	0.14
28	Landers_Coolwater_TR	Far Field	0.99	0.99	0.47	0.36	0.80	0.43
29	Landers_Coolwater_V	Far Field	0.15	0.15	0.10	0.12	0.13	0.08
30	Landers_YermoFireStation_270	Far Field	0.42	0.42	0.37	0.24	0.98	0.24
31	Landers_YermoFireStation_360	Far Field	0.17	0.17	0.20	0.11	0.46	0.08
32	Landers_YermoFireStation_V	Far Field	0.07	0.07	0.09	0.05	0.24	0.04
33	Northridge1_Beverlyhills12520_35	Far Field	0.35	0.35	0.34	0.22	0.39	0.21
34	Northridge1_Beverlyhills12520_125	Far Field	0.57	0.57	0.30	0.27	0.15	0.14
35	Northridge1_Beverlyhills12520_V	Far Field	0.15	0.15	0.12	0.11	0.18	0.07
36	Northridge1_Beverlyhills14145_09	Far Field	0.72	0.72	0.59	0.42	1.02	0.30
37	Northridge1_Beverlyhills14145_279	Far Field	1.61	1.61	0.85	0.53	1.01	0.60
38	Northridge1_Beverlyhills14145_V	Far Field	0.31	0.31	0.29	0.29	0.19	0.17
39	Northridge1_CanyonCountryWlostCanny_00	Far Field	1.36	1.36	0.44	0.47	0.61	0.52
40	Northridge1_CanyonCountryWlostCanny_270	Far Field	0.58	0.58	0.58	0.41	0.39	0.27
41	Northridge1_CanyonCountryWlostCanny_V	Far Field	0.14	0.14	0.12	0.13	0.28	0.10
42	KobeJapan_NishiAkashi_00	Far Field	0.59	0.59	0.40	0.41	0.38	0.25
43	KobeJapan_NishiAkashi_90	Far Field	0.71	0.71	0.61	0.37	0.31	0.20
44	KobeJapan_NishiAkashi_V	Far Field	0.21	0.21	0.13	0.15	0.12	0.10

`

45	KobeJapan_ShinOsaka_00	Far Field	0.46	0.46	0.41	0.29	0.54	0.20
46	KobeJapan_ShinOsaka_90	Far Field	0.44	0.44	0.43	0.37	0.35	0.20
47	KobeJapan_ShinOsaka_V	Far Field	0.11	0.11	0.06	0.08	0.13	0.05
48	KocaeliTurkey_Arcelik_00	Far Field	0.14	0.14	0.12	0.07	0.15	0.04
49	KocaeliTurkey_Arcelik_90	Far Field	0.12	0.12	0.15	0.08	0.22	0.06
50	KocaeliTurkey_Arcelik_V	Far Field	0.09	0.09	0.05	0.05	0.06	0.03
51	KocaeliTurkey_Duzce_180	Far Field	0.51	0.51	0.36	0.36	0.48	0.27
52	KocaeliTurkey_Duzce_270	Far Field	0.61	0.61	0.46	0.31	0.81	0.27
53	KocaeliTurkey_Duzce_V	Far Field	0.12	0.12	0.14	0.07	0.18	0.05
54	ChiChiTaiwan_CHY101_E	Far Field	0.51	0.51	0.60	0.30	0.65	0.23
55	ChiChiTaiwan_CHY101_N	Far Field	1.80	1.80	0.79	0.36	1.42	0.61
56	ChiChiTaiwan_CHY101_Vertical	Far Field	0.11	0.11	0.13	0.08	0.24	0.05
57	ChiChiTaiwan_CHY045_E	Far Field	0.56	0.56	0.37	0.37	0.22	0.19
58	ChiChiTaiwan_CHY045_N	Far Field	0.52	0.52	0.53	0.49	0.29	0.21
59	ChiChiTaiwan_CHY045_Vertical	Far Field	0.23	0.23	0.24	0.20	0.29	0.14
60	DuzceTurkey_Bolu_00	Far Field	0.88	0.88	0.49	0.52	0.72	0.37
61	DuzceTurkey_Bolu_90	Far Field	1.75	1.75	1.14	0.48	0.48	0.78
62	DuzceTurkey_Bolu_Vertical	Far Field	0.10	0.10	0.12	0.08	0.20	0.05
63	Manjillran_Abbar_L	Far Field	0.40	0.40	0.46	0.33	0.31	0.16
64	Manjillran_Abbar_T	Far Field	0.59	0.59	0.43	0.31	0.50	0.16
65	Manjillran_Abbar_V	Far Field	0.48	0.48	0.36	0.25	0.67	0.19
66	HectorMine_Hector_00	Far Field	0.30	0.30	0.27	0.19	0.40	0.13
67	HectorMine_Hector_90	Far Field	0.67	0.67	0.25	0.30	0.45	0.26
68	HectorMine_Hector_V	Far Field	0.15	0.15	0.16	0.08	0.20	0.05
69	ImperialValley06_Chihuaua_12	Near Field	0.42	0.42	0.36	0.35	0.32	0.22
70	ImperialValley06_Chihuaua_282	Near Field	0.50	0.50	0.51	0.35	0.55	0.27
71	ImperialValley06_Chihuaua_V	Near Field	0.07	0.07	0.08	0.05	0.06	0.04
72	ImperialValley06_ElCentroArray6_140	Near Field	0.54	0.54	0.64	0.33	1.13	0.29
73	ImperialValley06_ElCentroArray6_230	Near Field	1.21	1.21	0.51	0.32	1.83	0.39
74	ImperialValley06_ElCentroArray6_V	Near Field	0.50	0.50	0.34	0.24	0.52	0.20
75	ImperialValley06_ElCentroArray7_140	Near Field	0.42	0.42	0.69	0.30	0.56	0.20
76	ImperialValley06_ElCentroArray7_230	Near Field	2.01	2.01	1.02	0.52	1.52	0.78
77	ImperialValley06_ElCentroArray7_V	Near Field	0.25	0.25	0.16	0.16	0.31	0.10
78	ImperialValley06_BondaCorner_140	Near Field	0.07	0.07	0.04	0.05	0.02	0.03
79	ImperialValley06_BondaCorner_230	Near Field	0.11	0.11	0.13	0.08	0.09	0.06
80	ImperialValley06_BondaCorner_V	Near Field	0.00	0.00	0.00	0.00	0.00	0.00
81	IrpiniaItaly_Sturno_00	Near Field	0.37	0.37	0.29	0.27	0.42	0.20
82	IrpiniaItaly_Sturno_230	Near Field	0.33	0.33	0.35	0.19	0.77	0.14
83	IrpiniaItaly_Sturno_V	Near Field	0.14	0.14	0.11	0.09	0.26	0.06
84	NahanniCanada_Site1_10	Near Field	0.30	0.30	0.40	0.38	0.47	0.16
85	NahanniCanada_Site1_280	Near Field	0.41	0.41	0.42	0.26	0.38	0.17
86	NahanniCanada_Site1_V	Near Field	0.37	0.37	0.45	0.34	0.32	0.17
87	NahanniCanada_Site2_240	Near Field	0.28	0.28	0.21	0.30	0.17	0.15
88	NahanniCanada_Site2_330	Near Field	0.47	0.47	0.38	0.32	0.24	0.19
89	SuperstitionHills02_ParachuteTestSite_225	Near Field	3.26	3.26	1.24	0.60	1.61	1.12
90	SuperstitionHills02_ParachuteTestSite_315	Near Field	0.45	0.45	0.48	0.32	0.58	0.22
91	LomaPrieta_Bran_00	Near Field	0.67	0.67	0.72	0.49	0.45	0.34
92	LomaPrieta_Bran_90	Near Field	1.45	1.45	0.94	0.49	0.61	0.59
93	LomaPrieta_Bran_V	Near Field	0.23	0.23	0.18	0.13	0.21	0.08
94	LomaPrieta_Corralitos_00	Near Field	1.28	1.28	0.61	0.43	0.43	0.49
95	LomaPrieta_Corralitos_90	Near Field	0.68	0.68	0.61	0.52	0.69	0.29

`

96	LomaPrieta_Corralitos_V	Near Field	0.18	0.18	0.24	0.13	0.17	0.09
97	LomaPrieta_SaratogaAloha_00	Near Field	0.83	0.83	0.37	0.32	0.63	0.42
98	LomaPrieta_SaratogaAloha_90	Near Field	0.31	0.31	0.20	0.21	0.33	0.15
99	LomaPrieta_SaratogaAloha_V	Near Field	0.20	0.20	0.27	0.14	0.30	0.10
100	ErzicanTurkey_Erzincan_EW	Near Field	1.17	1.17	0.63	0.43	0.68	0.45
101	ErzicanTurkey_Erzincan_NS	Near Field	1.91	1.91	0.85	0.37	1.64	0.70
102	ErzicanTurkey_Erzincan_V	Near Field	0.18	0.18	0.13	0.12	0.27	0.08
103	CapeMendocino_CapeMendocino_00	Near Field	1.22	1.22	0.60	0.69	0.99	0.54
104	CapeMendocino_CapeMendocino_90	Near Field	0.25	0.25	0.31	0.18	0.48	0.10
105	CapeMendocino_CapeMendocino_V	Near Field	0.50	0.50	0.39	0.20	0.95	0.15
106	CapeMendocino_Petrolia_00	Near Field	1.05	1.05	0.67	0.54	0.44	0.41
107	CapeMendocino_Petrolia_90	Near Field	1.44	1.44	0.92	0.72	1.21	0.51
108	CapeMendocino_Petrolia_V	Near Field	0.14	0.14	0.13	0.12	0.18	0.09
109	Landers_Lucerne_260	Near Field	1.54	1.54	0.73	0.29	1.99	0.46
110	Landers_Lucerne_345	Near Field	0.41	0.41	0.30	0.23	0.34	0.17
111	Landers_Lucerne_V	Near Field	0.20	0.20	0.24	0.17	0.66	0.14
112	Northridge01_Lasepulveda_270	Near Field	1.56	1.56	1.56	1.09	0.63	0.80
113	Northridge01_Lasepulveda_360	Near Field	0.67	0.67	0.71	0.49	0.60	0.40
114	Northridge01_Lasepulveda_V	Near Field	0.61	0.61	0.23	0.19	0.36	0.22
115	Northridge01_1765SaticoySt_90	Near Field	0.44	0.44	0.36	0.26	0.53	0.19
116	Northridge01_1765SaticoySt_180	Near Field	0.99	0.99	1.04	0.40	0.93	0.36
117	Northridge01_RinaldiReceivingSta_228	Near Field	2.02	2.02	2.27	1.92	1.43	0.97
118	Northridge01_RinaldiReceivingSta_318	Near Field	0.67	0.67	0.90	0.48	1.00	0.33
119	Northridge01_RinaldiReceivingSta_V	Near Field	0.32	0.32	0.36	0.43	0.28	0.18
120	Northridge01_SylmarOliveView_90	Near Field	1.75	1.75	1.19	0.81	1.50	0.83
121	Northridge01_SylmarOliveView_360	Near Field	1.60	1.60	0.87	0.78	1.15	0.60
122	Northridge01_SylmarOliveView_V	Near Field	0.24	0.24	0.29	0.18	0.24	0.14
123	KocaeliTurkey_Izmit_90	Near Field	0.40	0.40	0.21	0.25	0.46	0.12
124	KocaeliTurkey_Izmit_180	Near Field	0.27	0.27	0.16	0.19	0.29	0.12
125	KocaeliTurkey_Izmit_V	Near Field	0.08	0.08	0.09	0.07	0.12	0.04
126	KocaeliTurkey_Yamica_30	Near Field	0.38	0.38	0.44	0.29	0.72	0.20
127	KocaeliTurkey_Yamica_60	Near Field	0.31	0.31	0.42	0.35	0.66	0.16
128	KocaeliTurkey_Yamica_V	Near Field	0.19	0.19	0.26	0.12	0.56	0.08
129	ChiChiTaiwan_TCU065_E	Near Field	2.23	2.23	0.84	0.59	1.79	1.00
130	ChiChiTaiwan_TCU065_N	Near Field	1.66	1.66	0.72	0.49	1.70	0.50
131	ChiChiTaiwan_TCU065_V	Near Field	0.35	0.35	0.38	0.20	1.22	0.19
132	ChiChiTaiwan_TCU067_E	Near Field	1.27	1.27	0.83	0.41	1.58	0.38
133	ChiChiTaiwan_TCU067_N	Near Field	0.85	0.85	0.56	0.39	0.63	0.23
134	ChiChiTaiwan_TCU067_V	Near Field	0.24	0.24	0.24	0.14	0.35	0.10
135	ChiChiTaiwan_TCU084_E	Near Field	5.90	5.90	3.98	2.06	1.89	2.76
136	ChiChiTaiwan_TCU084_N	Near Field	1.25	1.25	0.96	0.43	0.69	0.52
137	ChiChiTaiwan_TCU084_V	Near Field	0.59	0.59	0.48	0.30	0.29	0.24
138	ChiChiTaiwan_TCU102_E	Near Field	1.95	1.95	0.79	0.31	1.69	0.77
139	ChiChiTaiwan_TCU102_N	Near Field	0.60	0.60	0.30	0.27	0.68	0.26
140	ChiChiTaiwan_TCU102_V	Near Field	0.19	0.19	0.20	0.12	0.51	0.08
141	DuzceTurkey_Duzce_180	Near Field	1.17	1.17	0.70	0.36	0.38	0.48
142	DuzceTurkey_Duzce_270	Near Field	1.55	1.55	0.65	0.53	1.60	0.61
143	DuzceTurkey_Duzce_V	Near Field	0.10	0.10	0.11	0.10	0.18	0.07
144	DenaliAlaska_TAPSPumpStation10_47	Near Field	1.30	1.30	0.92	0.41	2.10	0.45
145	DenaliAlaska_TAPSPumpStation10_317	Near Field	0.31	0.31	0.46	0.23	1.16	0.14
146	DenaliAlaska_TAPSPumpStation10_V	Near Field	0.20	0.20	0.22	0.16	0.45	0.11